Development and prospects of dedicated tracers for the molecular imaging of bacterial infections

A. Bunschoten,[#,†] M. M. Welling,[#,†] M. F. Termaat,[‡] M. Sathekge,[§] F. W. B. van Leeuwen[†*]

[†] Department of Radiology, Interventional Molecular Imaging Laboratory, Leiden University Medical Center, Leiden, The Netherlands

[‡] Department of Trauma Surgery, Leiden University Medical Center, Leiden, The Netherlands

[§] Department of Nuclear Medicine, University of Pretoria & Steve Biko Academic Hospital, Pretoria, South Africa

Author information

Corresponding Author

* C2-S-204, Albinusdreef 2, 2333 ZA, Leiden, the Netherlands,

  Tel.: +31715266029. E-mail address: F.W.B.van_leeuwen@lumc.nl

Author contributions

# Equal contribution.

Abstract:

Bacterial infections have always been, and still are, a major global healthcare problem. For accurate treatment it is of upmost importance that the location(s), severity, type of bacteria, and therapeutic response can be accurately staged. Similar to the recent successes in oncology, tracers specific for molecular imaging of the disease may help advance the patient management. Chemical design and bacterial targeting mechanisms are the basis for the specificity of such tracers. The aim of this review is to provide a comprehensive overview of the molecular imaging tracers developed for optical and nuclear identification of bacteria and bacterial infections. Hereby we envision that such tracers can be used to diagnose infections and aid their clinical management. From these compounds we have set-out to identify promising targeting mechanisms and select the most promising candidates for further development.

Introduction

Since the beginning of the last century antibiotics have been developed and used to treat bacterial infections, e.g. penicillins, quinolones and glycopeptides. Despite the success of these compounds, bacterial infections are still a serious global healthcare problem. Tuberculosis is the most prominent example causing an estimated 1.5 million deaths in 2009 (table 1).[1]

In most patients bacterial infections are only identified when they have reached a systemic stage. Alternatively, the disease can become apparent when it has resulted in anatomical damage evident from clinical symptoms and/or via anatomical imaging e.g. X-ray, computed tomography (CT) and/or magnetic resonance imaging (MRI).[2] We reason that early and molecular diagnosis of

bacterial infections has the potential to allow optimization of treatment regimes. A prerequisite for such molecular diagnosis are imaging agents that can specifically accumulate in or around bacteria (scheme 1B). While the applications of molecular imaging are showing success in e.g. oncology, there still is a shortness of effective molecular imaging approaches for bacterial infections. In our view, molecular imaging approaches for bacterial infections have the potential to i) discriminate bacterial infections from sterile inflammation, ii) visualize the anatomical spread of infections, iii) identify the type of bacteria to select the best antimicrobial therapy, and iv) allow therapy monitoring.

Several unique molecular characteristics have been exploited to specifically target bacteria (summarized in scheme 1A). Especially the (negatively charged) bacterial membrane, excreted and membrane bound enzymes and receptors, intracellular enzymes and the DNA synthesis and translational machinery are specifically targeted. Next to this, passive internalization and intracellular entrapment can yield specific accumulation in bacteria. To achieve such targeting, and be suitable for clinical diagnostics, chemical entities have to fulfill a number of requirements. They should: 1) be non-toxic for the host, 2) target bacterial infections or produce a detectable signal upon interaction with bacteria, 3) penetrate rapidly into the infected area, and 4) emit a signal that allows in vivo identification.

Table 1.

Scheme 1.

For the visualization of bacterial infections there are two main routes of tracer administration, namely intravenous (IV) injection or a topical (local) administration. Whole body diagnostics of bacterial infections requires intravenous injection followed by 3D nuclear imaging technologies such as single-photon emission computed tomography (SPECT) and positron emission tomography (PET) preferably combined with CT or MRI for anatomical reference.[7] SPECT and PET imaging requires the incorporation of a radiolabel on the chemical moieties used to target the bacteria. Alternatively, superficial identification of bacterial infections and their spread e.g. during the surgical removal of infected prosthetics would benefit from fluorescence based identification.[8-10] This relatively unexplored approach can be accomplished after IV administration of a fluorescent tracer, but could also benefit from the topical introduction of (activatable) imaging tracers.

The technical aspects of nuclear and optical imaging of non-specific infection/inflammation imaging and the tracers currently used in the clinic have been reviewed by Signore et al,[11] and Dorward et al.[12] Regarding the current clinical state of the art, a number of nuclear imaging tracers are applied for non-invasive visualization of inflammations and infections, being ^{67}Ga-citrate (the oldest tracer),[13,14] its PET counterpart ^{68}Ga-citrate,[15-17] and a variety of radiolabeled leukocytes.[18-24]

Unfortunately these tracers accumulate in areas with sterile inflammations, infections, tissue regeneration, and cancerous lesions, making them non-specific for bacterial imaging.

Here we summarize the most well investigated classes of bacterial tracers, as well as –in our view- high potential bacterial imaging approaches.

Methods:

We performed an extensive literature research to identify bioactive compounds, conjugated to fluorescent or radioactive labels, designed for the imaging of bacterial infections. The identified compounds are classified on their general structure and targeting mechanism. The main families are the zinc(II)-dipicolylamine (Zn-DPA) tracers, the antimicrobial peptides, the antibiotics, the activatable tracers and the proteins. To provide a comprehensive overview of the different imaging tracers described in the literature, the chemical structures of the compounds have been added in the supporting information. The numbering of the compounds in the supporting information has been used in the main review. The reported bacterial specificity and uptake in infected tissues, indicated by the target to non-target (T/NT) ratios of the different compounds (also see the supporting information) were used to compare the different imaging tracers and select the most optimal chemical designs for molecular bacterial imaging strategies.

Most widely studied bacteria specific tracers

Zn-DPA

The negatively charged lipopolysaccharide and carbohydrate residues located in the outer membrane of both gram-positive and gram-negative bacteria are a potential target for imaging tracers. The positively charged metal complex zinc(II)-dipicolylamine (Zn-DPA) interacts with these negatively charged membranes (scheme 1A). This interaction facilitates discrimination between negatively charged bacterial membranes and neutrally charged membranes of mammalian cells. The Zn-DPA moiety facilitates conjugation to several types of labels, although the research has mainly focused on fluorescent labels.

Labeling methods

Imaging agents based on dimers, tetramers and multimers of Zn-DPA have been developed. A dimer was conjugated via a short polyethylene glycol spacer (PEG) to dansyl (**1**) or directly to fluorescent anthracene (**2**).[25] A near-infrared (NIR) version of this tracer was developed by coupling a NIR-cyanine dye to the Zn-DPA moieties via a short alkyl spacer (fig. 1B; **3**). This compound (commercialized as PSVue®794) demonstrated membrane staining of bacterial cells both in vitro and in murine infection models.[26-28] A Cy5-labeled Zn-DPA tracer (**4**) was applied to study the binding to

bacterial membranes in more detail via förster resonance energy transfer (FRET) interactions with a fatty acid conjugated Cy3-derivative that was incorporated in a bacterial-like lipid bilayer vesicle.[29]

A second generation of the Zn-DPA moiety, based on 2,6-bis(zinc(II)-dipicolylamine)phenoxide (**5**), was developed by DiVittorio et al.[30] The tyrosine core of this targeting moiety enabled its incorporation in peptides and offered an additional reactive group for the attachment of moieties to fine-tuning the chemical and biological behavior of the synthesized tracers. Based on this concept, the 7-nitrobenz-2-oxa-1,3-diazol-4-yl-label (NBD) labeled version was synthesized and tested. Unfortunately no comparison was made with the first generation tracers.

To develop Zn-DPA targeted tracers with brighter (higher quantum yield) and more photostable dyes, Johnson et al. selected a squaraine dye.[31] Although squaraine dyes are chemically unstable in biological environments, incorporation into a rotaxane moiety to form a sterical barrier improved their stability dramatically. The squaraine rotaxane, labeled with four Zn-DPA moieties (**6**), proved to be equally bright to a Cy5-labeled version, but was found to be more photostable ($t_{1/2}$ of 1080 s and 11 s respectively). This increased photostability allowed the generation of real-time fluorescence-microscopy movies of dividing bacteria incubated with the imaging tracer.[31] Squaraine dyes, protected by two different rotaxanes (**6, 7**), allowed in vivo visualization of infections.[32]

The Zn-DPA targeting moiety has also been applied on nanoparticles presenting multiple copies of the targeting moiety. Biotin conjugated to Zn-DPA (**8**) facilitated binding to streptavidin coated quantum dots (λ_{em} 565, 655 and 800 nm).[33] A radioactive imaging agent containing the Zn-DPA targeting moiety has also been developed. Herefore, biotinylated Zn-DPA and biotinylated ^{111}In-DOTA (**9**) were combined on streptavidin in a 1:1:1 ratio.[34]

Bacterial imaging studies

From a chemical point of view, the targeting moieties of the above-described tracers are exactly the same, except for compound **5.** This offers the opportunity to compare the effect of the different imaging labels on the biological performance of the tracers. All compounds, except for the Zn-DPA labeled quantum dots (**8**) were able to bind to both gram-positive and gram-negative bacteria in vitro and in vivo. The quantum dots showed selectivity for gram-negative bacteria because their relatively large size (15-20 nm) prevented them from passing through the cell wall of gram-positive bacteria thereby limiting the interactions with the negatively charged membrane.[33]

For compounds **3**, **4**, **6** and **7**, the T/NT ratio in vivo was measured at several time points after IV injection. Thakur et al. reported a maximum T/NT ratio of 6.6 for a bacterial infection in the thigh of mice and a T/NT = 3.2 for a sterile inflammation at 3 h post injection of compound **3** (Fig. 1A).[28] Cy5-labeled Zn-DPA derivative **4** showed the fastest clearance and reached a T/NT ratio of 4.2 (6 h post injection); Little residual fluorescence was present at 24 h post injection.[29] A clear difference in bacterial imaging was seen between the lipophilic squaraine rotaxane **7** and the more hydrophilic squaraine rotaxane **6**. Tracer **6** reached a T/NT ratio of 6 (6 h post injection) and this ratio decreased

to 4 (21 h post injection), while the accumulation of **7** steadily increased to a T/NT ratio of 4 (12 h post injection) and remained steady till 21 h post injection.[32] The non-specific uptake in various organs was also significantly higher for the more lipophilic compound **7**. The radiolabeled Zn-DPA/^{111}In-DOTA-biotin-streptavidin complex reached a T/NT ratio of 2.8 (22 h post injection).

Although the usefulness of the Zn-DPA targeting moiety for bacterial imaging has been demonstrated in several studies, its affinity for negatively charged structures has also been applied to target apoptotic cells, which become more negatively charged during the onset of apoptotic and necrotic processes.[35-40] In this respect, also necrotic processes related to tumors have been imaged with Zn-DPA targeting moieties, because tumor genesis often involves dying cells (T/NT ratio of 2.2 at 24h post injection).[41]

Figure 1

Summary

Promising results have been described with the widely studied fluorescently and radioactive labeled Zn-DPA-derivatives. Both in vitro and in vivo, they have been able to label bacteria and image bacterial infections. However, the specificity remains an issue. Zn-DPA targets negatively charged cells, so this moiety targets also dead and dying cells such as in apoptotic and necrotic processes, which appear in both infectious and inflammatory processes. For that reason we think that Zn-DPA-derivatives are not the best candidates for infection specific imaging.

Antimicrobial peptides

Antimicrobial peptides (AMPs) are short polypeptides (12-50 residues) that form a part of the innate immune system in all classes of life. Generally, these antimicrobial peptides form amphipathic helices that bind to the bacterial membrane, mostly based on electrostatic interactions, and damage its integrity (scheme 1A). These peptides demonstrate a broad-spectrum activity against both gram-positive and gram-negative bacterial strains. The interaction of these compounds with bacterial membranes makes them promising tools for targeting bacterial infections.

Labeling methods

Few fluorescently labeled AMPs have been described in the literature and they have not yet been applied broadly for infection imaging. Fluorescein-labeled Buforin II (**10**) and magainin 2 (**11**) were synthesized via an isothiocyanate coupling. The exact position of the label was not specified by the authors, as multiple free amines (N-terminus and lysine residues) were available for reaction with the isothiocyanate. Fluorescence imaging of labeled bacteria revealed internalization of Buforin II, while magainin 2 remained extracellular and caused lysis of the bacterial membrane.[42]

Cy5-labeled antimicrobial peptides cecropin P1 (**12**), SMAP29 (**13**) and PGQ (**14**) were synthesized by the selective introduction of a Cy5-maleimide on C-terminal cysteine residues, which left the pharmacophore of the AMP intact. These fluorescently labeled AMPs were applied for the direct labeling of bacteria or to replace antibodies in an in vitro immuno-magnetic bead biosensor.[43]

Bac7$_{1-35}$ (**15**), labeled with bodipy-maleimide on a C-terminal cysteine residue, was used to evaluate bacterial penetration in vitro using fluorescence-activated cell sorting (FACS).[44] Furthermore, Bac7$_{1-35}$ was labeled with Alexa680-maleimide and studied for its antibacterial action in vivo. The distribution in healthy mice was studied by quantifying the fluorescence signal, but no targeting experiments in infected mice were conducted.[45]

Nisin (**16**), an antimicrobial peptide produced by bacteria to kill competing strains (bacteriocin), was labeled with 5-(aminoacetamido)fluorescein (AAA-Flu) on a free C-terminal carboxylic acid. This fluorescent derivative was applied to elucidate its mode of action on the bacterial cell wall synthesis.[46]

Nuclear labeled AMPs have been applied for the imaging of infections. We labeled human neutrophil peptide 1 (HNP-1; **17**), a natural defensin, human β-defensin-3 (HBD-3; **18**) and the synthetic peptide lactoferrin 1-11 (^{99m}Tc-hLF 1-11; **19**), derived from human lactoferrin with ^{99m}Tc via direct labeling.[47-50] Histatins, antimicrobial peptides found in human saliva, were studied for their potential in bacterial imaging. ^{99m}Tc-labeled synthetic derivatives of histatin 5 and dimers thereof (**20 a-g**) were developed. The in vitro antimicrobial activity was improved by forming histatin dimers, but these constructs did neither show improved in vivo killing of bacteria nor improved visualization of bacterial infections.[51]

The most studied antimicrobial peptide for infection imaging is ubiquicidin 29-41 (UBI$_{29-41}$; **22a**). This peptide sequence was selected from the complete sequence of the human antimicrobial peptide ubiquicidin (6.7 kDa). Generally, ^{99m}Tc is introduced on UBI$_{29-41}$ via direct labeling (fig. 2B; **22b**).[52] To evaluate the different approaches to coordinate ^{99m}Tc to UBI$_{29-41}$ several chelate-conjugated UBI$_{29-41}$ peptides were developed. They were compared with the direct labeling approach regarding binding to bacteria and imaging of bacterial infections. Conjugation of mercaptoacetyltriglycine (MAG$_3$) to UBI$_{29-41}$ (**22c**) was performed by coupling of tetrafluorophenol-activated ^{99m}Tc-MAG$_3$ to free amines in UBI$_{29-41}$. The resulting imaging agent showed similar bacterial binding capacity as observed for directly labeled UBI$_{29-41}$.[53] The chelates 6-hydrazinonicotinic acid (HYNIC) and diaminedithiol (N$_2$S$_2$) were coupled N-terminally to UBI$_{29-41}$ (**22d,e**).[54]

Visentin et al. introduced ^{123}I on the tyrosine residue present in the UBI-sequence (**22f**).[53] The first UBI$_{29-41}$ PET tracer was developed by introducing ^{18}F via the coupling of N-succinimidyl-4-[^{18}F]fluorobenzoate to the free amines in UBI$_{29-41}$ (**22g**).[55] Unfortunately labeling via the lysine residues in the peptide sequence reduced the binding to S. aureus. Conjugation selectively to the N-terminus instead of the lysine residues could prevent such interference with the biological activity of the AMP.[54] Ebenhan et al. developed an UBI-based PET tracer ^{68}Ga-NOTA-UBI$_{30-41}$ (**22h**) with the

chelate conjugated to the N-terminus.[56] Recently a NIR-fluorescently labeled version of UBI$_{29-41}$ was developed and tested in mice with bacterial infections.[57]

The fast clearance of peptides can hamper their application in vivo. Improved in vivo half-life for AMPs has been realized by applying peptidomimetics. Seo et al. synthesized amphipathic helical antimicrobial peptides consisting of peptoid building blocks. These are amino acids with the functional side chains connected to the amine nitrogen instead of the Cα of the amino acid backbone, which results in a reduced proteolytic susceptibility. ^{64}Cu-DOTA labeled versions of these antimicrobial peptoids (2**1a-c**) were developed. Although, the authors did not report any bacterial targeting, they showed greater in vivo stability and slower clearance compared to normal antimicrobial peptides.[58]

Pretargeting

In contrast to eukaryotic cells, bacteria can metabolize and utilize D-amino acids. Kuru et al. used fluorescently labeled D-amino acids (**23a-d**), which were incorporated in the peptidoglycan layer of all studied bacteria.[59] By introducing R-propagylglycine or R-2-amino-3-azidopropanoic acid (**24a-b**) to growing bacteria, either in vitro or to L. monocytogenes infected macrophages, the azide or alkyne moiety was incorporated in the peptidoglycan layer. These reactive groups could be labeled in a second step by complimentary labeled fluorophores via the Cu(I)-assisted or strain-promoted click reaction and the Staudinger ligation.[59,60]

Bacterial imaging studies

Fluorescently labeled Bac7$_{1-35}$ has been applied in vivo to study the biodistribution in healthy mice, showing fast clearance mainly via the kidneys.[45] The biodistribution of a NIR-fluorescently labeled UBI$_{29-41}$ peptide was tested in infected mice.[57] Unfortunately, the dye seemed to influence the distribution of the construct to a large degree, resulting in a similar distribution for the dye alone compared to the fluorescently labeled UBI$_{29-41}$. The other fluorescently labeled AMPs have not yet been applied in vivo.

Radioactively labeled AMPs have been widely applied in infection imaging and some tracers have even been tested successfully in patients. ^{99m}Tc-HNP-1 (**17**) showed rapid imaging (5-15 min post injection) of infected thigh muscles in mice with a T/NT ratio of 2.[47] HBD-3 (**18**) reached T/NT ratios between 2.5-3 in the infected thigh muscle model.[50] For ^{99m}Tc-hLF 1-11 (**19**) different routes of administration were evaluated. After intravenous, intraperitoneal and subcutaneous administration ^{99m}Tc-hLF 1-11 reached a T/NT ratio of 3.5-4 (1 h post injection) while oral administration resulted in a T/NT ratio of 2.5.[49] Unfortunately, human lactoferrin, recombinant lactoferrin and peptide fragments thereof accumulated in the liver, kidneys and intestine, making these tracers less suitable for imaging infections in the abdominal area.[48,61,62] Of the histatin variants, the best T/NT ratio was 4.5 (1 h post

injection) for the dimeric Dh5 (**20e**) in a S. aureus thigh muscle infection, but no further research has been reported[51]

UBI$_{29-41}$ (**22a**) has extensively been studied, both in the preclinic and the clinic. The selectivity of the peptide sequence for infections was determined in vivo by competition studies with both an unlabeled UBI$_{29-41}$ and a scrambled version of UBI$_{29-41}$ peptide.[63] For ^{99m}Tc-UBI$_{29-41}$ T/NT ratios between 2-3.5 (1-2 h post injection) were reported in mice with an infected thigh muscle..[48,64] In rabbits with infected thigh muscles, T/NT ratios between 2-5 (1-4 h post injection) were reported.[61,65] ^{99m}Tc-UBI$_{29-41}$ has also been applied for the diagnosis of bacterial endocarditis, acute postoperative prosthetic joints infection and antibiotic therapy monitoring.[66-69] In patients, ^{99m}Tc-UBI$_{29-41}$ (**22b**) has been evaluated in bone, soft tissue, prosthetic and diabetic foot infections and in fever of unknown origin (FUO), resulting in T/NT ratios of 2.1-2.8 (0.5-2 h post injection) (Fig. 2A).[70-74] Furthermore, ^{99m}Tc-UBI$_{29-41}$ has successfully been applied for antibiotic therapy monitoring.[75] UBI$_{29-41}$ labeled with ^{99m}Tc-HYNIC (**22d**) has also been evaluated in patients, resulting in similar T/NT ratios as reported for directly ^{99m}Tc-labeled UBI 29-41.[76]Recently the biodistribution of ^{68}Ga-NOTA-UBI$_{30-41}$ was evaluated in healthy vervet monkeys, which showed rapid renal clearance without accumulation of radioactivity in the major organs.[56]

Figure 2.

Summary

Antimicrobial peptides have proven to be effective tracers for imaging bacterial infections in animals and in patients making them 'high potential' candidates for further developments. Especially UBI$_{29-41}$ has extensively been studied, for most other AMPs only limited data is available. Due to the relatively high background uptake, the reported T/NT ratios are generally ranging between 2 and 3, which has to be improved to make them clinically valuable. Additionally, the fast (renal) clearance and proteolysis of peptides in vivo can be an obstacle as it limits the circulation time of the tracer and the time window available for both pre-interventional and intra-interventional imaging. The application of peptidomimetics has the potential to increase the resistance against proteolysis and elongate the in vivo half-life.

Carbohydrates

Bacteria require carbohydrate building blocks for their replication, membrane synthesis, virulence and energy demand. Next to this, bacteria also interact with carbohydrates on cellular membranes to pass barriers or infiltrate cells.[77] Therefore, specific carbohydrates are recognized and/or actively incorporated into bacteria or are taken up by passive internalization and further processed intracellular (scheme 1A). These mechanisms make carbohydrates possible targeting

moieties for imaging bacteria. By applying different carbohydrates, a selectivity for specific bacterial strains may be accomplished.

Labeling methods

In nature, carbohydrates are involved in low-affinity cell-cell interactions, but these interactions are effectively enhanced by the multivalency effect.[78] To mimic these multivalent interactions, water-soluble carbohydrate-functionalized fluorescent polymers (**25, 26**) were developed. A mannose functionalized polymer showed aggregation with E. coli via interaction with the FimH lectin, while FimH deficient bacteria or galactose/glucose functionalized polymers showed no aggregation.[79,80] Similar aggregation of bacteria and/or bacterial internalization of fluorescent nanocrystals (quantum dots; QDs) was observed with QDs (3.5-15 nm; em. 540-630 nm) coated with small molecules such as citrate-derivatives,[81] adenine-derivatives,[82] and mannose.[83] However, the value of these constructs for in vivo application is limited due to their large size.

Smaller analogues ranging from 1-7 monosaccharides have also been applied for bacterial imaging (**27-36**). Trehalose is a non-mammalian disaccharide that is incorporated in the membrane of mycobacteria by the trehalose mycolyltransesterase enzymes (Ag85 A-C).[84] These enzymes have a broad substrate selectivity and tolerated the attachment of a fluorescein moiety (**28**), which enabled the fluorescent labeling of M. tuberculosis in vitro.

2-deoxy-2-[^{18}F]fluoro-D-glucose ([^{18}F]FDG; **31**) is the clinical standard nuclear imaging agent for tumor imaging with positron emission tomography (PET). Due to its uptake in areas with increased metabolism, its applicability for infection imaging was also studied.[85-87] A ^{99m}Tc-labeled glucose derivative 1-thio-β-D-glucose 2,3,4,6-tetra-acetate (^{99m}Tc-TG; **32**) was developed and the interaction with bacteria was compared to that of [^{18}F]FDG.[88]

Aminosugars are building blocks for the synthesis of the peptidoglycan layer in both gram-positive and gram-negative bacterial strains. Martinez et al. introduced an ^{18}F-label into N-acetylglucosamine ([^{18}F]FAG; **33**) and demonstrated the possibility to discriminate between inflammation and bacterial infections in a rat muscle infection model.[89]

A very promising imaging agent for bacterial infections is the thymidine kinase substrate 1-(2'-deoxy-2'-fluoro-β-D-arabinofuranosyl)-5-iodouracil (FIAU; **34**). This substrate is phosphorylated intracellularly by many pathogenic bacteria, after which it is trapped within the bacterium. As FIAU is a poor substrate for the major human thymidine kinase (TK1) and therefore it may be selective for imaging bacterial infections. Both a gamma emitting [^{125}I]FIAU derivative as an positron emitting [^{124}I]FIAU (fig. 3C) have been developed and tested for infection imaging.[90-92] A similar ^{18}F-labeled compound, 3'-deoxy-3'-[^{18}F]fluorothymidine ([^{18}F]FLT; **35**) was developed by Jang et al.[93]

The glucose demand of bacteria can be targeted with maltodextrin-based imaging tracers (MDPs; **27**). Maltohexaose was labeled with a perylene or an IR786 label via the Cu(I)-catalyzed

click reaction (fig. 4B). The tracers were internalized specifically via the maltodextrin transport pathway where it is used as a source of glucose.[94]

Cyclodextrin is a ligand for the maltose-binding protein expressed by bacteria. Shukla et al. labeled 2-hydroxypropyl cyclodextrin with ^{99m}Tc (^{99m}Tc-HPβCD; **36**) by direct labeling. The biodistribution in rats was studied and bacterial infections in patients with knee prosthesis were imaged.[95]

Pretargeting

A carbohydrate based pretargeting approach for bacteria was described by Dumont et al. They provided gram-negative bacteria with 8-azido-8-deoxy-3-deoxy-D-mannooctulosonic acid (KDO-N$_3$; **30**), which is a ligand for CMP-KDO synthetase. Via this route KDO-N$_3$ was incorporated in the lipopolysaccharide layer. Next, an alkyne-conjugated Alexa488 (**30**) was introduced to react with the incorporated KDO-N$_3$ via the Cu(I)-catalyzed click reaction.[96] A similar approach was recently performed with azide derivatives of the above described disaccharide trehalose (**29a, b**).[97]

The advantage of a pretargeting approach is the minor chemical modification necessary for the primary targeting moiety, ensuring normal ligand binding and incorporation. In the second, step the imaging label is introduced and will react solely with the bacteria that have incorporated the primary targeting tracer. Both carbohydrates were effective in vitro. For in vivo experiments, the approach chosen by the authors will not be applicable because of the copper(I) required for the applied click reaction. A copper-free click reaction would be more appropriate for in vivo applications.[98]

Bacterial imaging studies

All events of increased glucose metabolism can cause increased uptake of [^{18}F]FDG (**31**), such as growth, immunological reactions, tissue repair, malignancies, and the presence of replicating pathogens.[99] A survey of the recent literature on the use of [^{18}F]FDG in detecting mycobacterium infections let to the conclusion that [^{18}F]FDG is not specific for bacterial infections.[100] Although [^{18}F]FDG was not capable of discriminating between different types of lesions that cause increased glucose uptake, this tracer was useful in antimicrobial therapy monitoring.[100]

In a combined application of [^{18}F]FDG and [^{11}C]PK11195, a macrophage binding compound, Ren et al. could discriminate between septic and aseptic loosening of implants in rats by comparing the T/NT ratios of both tracers.[101]

Although a higher accumulation in infections was observed with a ^{99m}Tc-labeled glucose derivative ^{99m}Tc-TG (**32**) compared to [^{18}F]FDG, this same increase was observed in tumors.[88] In contrast to [^{18}F]FDG, the fluorine labeled glucosamine [^{18}F]FAG (**33**) did show selectivity for bacterial infections in mice, resulting in a T/NT ratio of 2.8 for a bacterial infection and 1.4 for a turpentine oil induced inflammation (1 h post injection).[89]

Promising results have been obtained with FIAU (**34**). This nucleoside analog could image infections with bacterial strains that express TK1 or similar thymidine kinases. Bettegowda et al. injected ^{125}I-labeled FIAU in mice infected with several gram-positive and gram-negative bacterial strains. In S. aureus infected mice a T/NT ratio of 14 (24 h post injection) was reported indicating a high sensitivity.[90] Recently, this tracer was used to image diffuse lung infections in mice infected with E. coli. Bacteria infected lungs were specifically identified and they were able to detect bacteria at 10^9 CFU/mL.[92] Diaz et al. applied [124I]FIAU (**34**), a positron emitting variant, for the imaging of bacteria in patients with suspected musculoskeletal infections in knee joints and lower extremities. They reported accumulation of the tracer in all patients with confirmed bacterial infections and no significant accumulation was observed in a healthy control person or in a patient with a confirmed sterile inflammation (fig. 3A, B).[91] Peterson et al. recently showed the uptake of [14C]FIAU in common bacteria for which immune suppressed patients are more susceptible and showed a good uptake for most, except for P. aeruginosa.[102]

Figure 3

Jang et al. recently applied both [125I]FIAU and 3'-deoxy-3'-[18F]fluorothymidine [18F]FLT (**35**) for the detection of S. typhimurium in vitro and in infected mice. The uptake of [125I]FIAU in bacteria was significantly higher than the uptake of [18F]FLT, nevertheless both agents accumulated at the infected lesions with T/NT of 2.98 and 12.3 (1 h and 2 h post injection respectively).[93] However, [18F]FLT is also applied as a tool for measuring in vivo tumor cell proliferation, which makes this marker probably not bacteria specific.[103]

Maltohexaose (**27**) targets the glucose-uptake of bacteria, which resulted in intracellular accumulation up to millimolar concentrations.[94] In a mouse model inoculated with 10^7 CFU of viable E. coli in the thigh muscle a T/NT ratio of 26 was established (16 h post injection)(Fig. 4A). Moreover, a T/NT ratio of 2 was still achieved in mice infected with 10^5 CFU, indicating a high sensitivity. Uptake was shown in all tested strains: E. coli, P. aeruginosa, B. subtilis and S. aureus, which could make compound **27** a versatile tracer.

Figure 4.

The application of ^{99m}Tc-HPβCD as an infection specific tracer has been demonstrated by Shukla et al. After injection in rats, the ^{99m}Tc-HPβCD was mainly cleared via the kidneys. In patients it showed an increased uptake in an infected knee over a control knee. Unfortunately, no T/NT ratios were reported and very poor information was provided in this publication about the used compounds and performed studies, which made it hard to draw any conclusions regarding its usefulness in infection imaging.[95]

Summary

Carbohydrate tracers that accumulate in bacteria or bacterial membrane structures show great promise for the development of bacterial infection specific tracers. Especially trehalose (**28**, **29**) for M. tuberculosis imaging and the maltohexaose (**27**) and FIAU (**34**) for more general bacterial imaging are promising candidates for clinical translation.

Antibiotics

The largest group of targeting moieties that has been investigated for infection imaging are the antibiotics. These drugs interact with high affinity and specificity with bacterial structures and intracellular proteins and enzymes (scheme 1A). It is this specificity that theoretically makes them ideal targeting moieties. Various studies have been performed using radiolabeled or fluorescently labeled antibiotics.

Labeling methods

Until now, most fluorescently labeled antibiotics have been used to study the permeability of antibiotics into tissue, the synthesis of bacterial membranes and cell walls, and the interactions of the antibiotics with the bacterial membrane. Fluorescently labeled vancomycin, telavancin, polymyxin B (fig. 5B), penicillin G (bocillin), and ramoplanin (**37, 40, 43, 45, 46**) have been described.[44,104-107] All compounds were labeled on free amines using NHS-esters or isothiocyanates of fluorescein and/or bodipy. Using fluorescence imaging techniques these tracers revealed clear spots of increased labeling of or within the bacterial membrane (fig. 5A), indicating the sites of peptidoglycan synthesis or the presence of specific lipid structures. Dhanapal et al. developed a synthetic route towards fluorescent quinolones (**44**), which were able to label both gram-positive and gram-negative bacteria in vitro.[108] However, none of these fluorescently labeled antibiotics have, to our knowledge, been used for in vivo imaging of infections.

Figure 5.

Radioactive labeling is, generally speaking, a better choice for in vivo imaging applications with the relatively small sized antibiotics. Compared to labeling with large optical imaging labels, there is little to no effect of the nuclear labeling on the chemical structure. Multiple antibiotics have been radiolabeled to determine their biodistribution and several of them have been applied for infection imaging. For this purpose, direct labeling with ^{99m}Tc or incorporation of ^{18}F during synthesis are the most applied methods of labeling.

The major group of antibiotic tracers developed for infection imaging in (pre-)clinical settings are the fluoroquinolone antibiotics.[109-124] Ciprofloxacin is the best studied derivative of this class of

antibiotics and the ^{99m}Tc-labeled version has been commercialized as Infecton® for the imaging of infections (**81a**).

Several other classes of antibiotics have also been radiolabeled and used for infection imaging, such as cephalosporins,[125-133] aminoglycosides,[134,135] and several others.[134,136-144]

Singh et al. developed ^{99m}Tc-isoniazid (**76**), an antibiotic especially applied for treatment of TB. Radiolabeling was performed by the introduction of a thiol in the structure of isoniazid by reaction with 2-iminothiolane. This thiol facilitated the coordination of ^{99m}Tc to form a radiolabeled complex.[145] By coupling two isonicotinic acid hydrazides to DTPA a ^{99m}Tc-labeled dimeric version of isoniazid (^{99m}Tc-DTPA-bis(INH)) was created (fig. 6C; **77**).[146]

Next to fluorescently-labeled vancomycin (see above), this antibiotic has also been labeled with various radioisotopes. Perkins et al. radioiodonated vancomycin with ^{125}I in 1970, mainly to study the fate of the antibiotic in bacteria.[147] Furthermore, vancomycin has been labeled directly with ^{99m}Tc,[148] and [201]Tl (**38**).[149,150]

Pretargeting

Vancomycin has been applied in a pretargeting approach. The antibiotic was labeled with a trans-cyclooctene via the free amine on the carbohydrate moiety (**41**). After binding to bacteria, a magnetofluorescent nanoparticle (MFNP) with a tetrazine-moiety was added. This resulted in a reaction with the cyclooctene-vancomycine via the tetrazine-trans-cyclooctene ligation (TTCO) and subsequent visualization of the bacteria.[151] A similar experimental setup was carried out with daptomycin, although this was less successful due to poor binding and/or due to diminished reactivity towards the tetrazine conjugated MFNPs.

Bacterial imaging studies

Although many antibiotics have been radiolabeled and tested for infection imaging applications, most of them were not successful in doing so. Modest to low T/NT ratios were reported or similar T/NT ratios were observed for both bacterial infections and sterile inflammations, indicating that no discrimination could be made.

There are however some promising candidates within this class of imaging tracers, which we shortly discuss below. ^{99m}Tc-Cefepime (**70**), which binds to penicillin binding proteins (PBPs), demonstrated selective accumulation in an E. coli infected thigh muscle compared to a heat-killed E. coli and a turpentine oil induced inflammation in a rat model. A T/NT ratio of 8.4 (3 h post injection) compared to 4 and 3.3 respectively was reported.[131] High T/NT ratio of 7.3 for an MRSA infection and 1.2 for a sterile inflammation (90 min post injection) were obtained in rats with ^{99m}Tc-rifampicin (**72**).[137] The plant-derived ^{99m}Tc-pheophorbide-a (**73**) was able to discriminate between an infected and inflamed thigh muscle in rats with a T/NT ratio of 5.6 compared to 1.3 respectively (1 h post

injection).[138] However, the amount of accumulated dose of the tracers was very low (0.0017 %ID/g). Injection of [99mTc]-vancomycin (**38**) resulted in a T/NT ratio of 5 in S. aureus infected rats compared to a ratio of 1.5 for a sterile inflammation (1 h post injection).[148]

[99mTc]-Isoniazid (**76**) showed a T/NT ratio of 3.5 (24 h post-injection) and could discriminate between an S. aureus and an M. tuberculosis infection.[145] The combination of a 24 h imaging interval and the short half-life of [99mTc] (6h) required a high initial dose to obtain sufficient signal. The [99mTc]-labeled dimeric isonicotinic acid hydrazide (**77**) accumulated at TB-lesions in mice with T/NT ratios between 4.2-4.5 (1-24 h) and reached a ratio between 2.87 and 2.46 in 6 patients with extrapulmonary TB infections (1 h and 4 h post injection respectively)(fig. 6A, B).[146]

[[131I]]Linezolid (**79**), an antibiotic against gram-positive bacteria, showed the highest T/NT ratios of the above mentioned antibiotics. At 30 min post injection a T/NT ratio of 77.5 was reported for an S. aureus inflamed muscle in rats and a 14.9 ratio for a turpentine oil induced sterile inflammation.[143] However, no further studies were performed or imaging data were presented.

Figure 6.

The most extensively studied radiolabeled antibiotic is ciprofloxacin, of which the [99mTc]-labeled version was commercialized as Infecton® (**81a**). Its mode of action depends on blocking bacterial DNA replication by binding to DNA gyrase. Ciprofloxacin is a broad-spectrum antibiotic that is active against both gram-positive and gram-negative bacteria. After radiolabeling, this antibiotic could detect bacterial infections in both animal models and patients.[152-158]

However, also critical results have been reported; e.g. significant accumulation in non-infected prosthetic joints and the inability to discriminate between infected and aseptic osteoarticular disease in patients.[116,159-161] In a phase II clinical study Infecton® showed poor specificity and accuracy in patients with suspected osteomyelitis both at images taken 2 h and 24 h post injection.[162] Based on these results, the company Draxis health inc. decided in 2007 to stop the further development of Infecton®.

Since then several variants of ciprofloxacin with various radioisotopes or different methods of introducing them were developed. Langer et al. developed an [18F]-labeled ciprofloxacin (**81b**) designed for PET-studies. Unfortunately, infection specific imaging in patients with [[18F]]ciprofloxacin was not successful.[163,164] Zijlstra et al. introduced [18F] via the coupling with 4-[[18F]]fluoro-ω-bromo-acetophenone (**81c**), but no specific bacterial binding was observed with this tracer.[55] Sachin et al. developed two other [18F]-labeled derivatives of ciprofloxacin (**81d,e**) by introducing an alkylfluoride, resulting in good bacterial uptake into two E. coli strains, but no imaging studies were reported with this tracer.[165] Zhang et al. introduced a dithiocarbamate to chelate [99mTc] (**81f**) and reported accumulation in infected thigh muscle in mice.[166] Dahiya et al. introduced different chelators for [99mTc]

at several positions within ciprofloxacin (**81g-i**), which resulted in compounds with similar imaging characteristics compared to Infecton®.[167]

Summary

Although antibiotics are selective in killing bacteria, they are not always selective in targeting bacteria and do not accumulate at infected sites. In many imaging studies with nuclear labeled antibiotics, only small differences are reported in the T/NT ratios between infections and sterile inflammations or no comparison has been made with sterile inflammations at all. Only a small number of antibiotics have shown potential for in vivo infection imaging. However, antibiotic-based imaging tracers will be ineffective in drug-resistant strains and applying antibiotics in sub-therapeutical dosages causes increased mutagenesis and can lead to increased resistance against these antibiotics.[168]

Promising new approaches

Bacteriophages

Bacteriophages are viruses that exploit bacteria as host for their reproduction. After recognition of the outer layer (scheme 1A), the bacteria are infected and new bacteriophages are synthesized generally killing the bacteria in the process. This recognition of certain bacterial strains can make bacteriophages highly specific targeting moieties for bacterial infections.

Labeling methods

Genetically labeled bacteriophages were created by incorporation of green fluorescent protein (GFP) on the C- or N-terminus of the small outer capsid (SOC) proteins of the virus to image bacteria e.g. in sewage water.[169,170] Bacteriophages have been fluorescently labeled with fluorescent nucleic acid dyes SYBR gold and SYBR green I, after which they were used to target and label bacteria.[171,172] By combining immuno-magnetic isolation by antibody-coated magnetic beads with staining by bacteriophages, Goodridge et al. could reach very low detection limits (10^1-10^2 CFU/mL) of bacterial pathogens in food samples.[173] The success of this approach strongly depended on the specificity of the applied antibodies and bacteriophages. ^{99m}Tc-labeled bacteriophages were developed to image infections in mice. The phages were covalently labeled on free amines with NHS-MAG3 and thereafter radiolabeled with ^{99m}Tc.[174,175]

Pretargeting

Wu et al. developed a pretargeting method with bacteriophages, by generating bacteriophages that express the minor coat protein pIII with an additional tetracysteine tag at the N-terminus. After binding of the bacteriophage to the target bacteria, it could be labeled with a fluorigenic biarsenical dye.[176] Alternatively, Edgar et al. used the reproduction of bacteriophages by the target bacteria. The

applied bacteriophages contained a gene for the production of a biotinylated protein. And after production of the virus particles by the host, this protein could be targeted by streptavidin coated quantum dots.[177]

Bacterial imaging studies

Until now, none of these fluorescently labeled bacteriophages have been used for imaging bacterial infections in vivo, only for detecting bacteria in food or water samples.

With the radiolabeled bacteriophage M13 a higher accumulation was observed in an E. coli infected thigh muscle compared to an inflamed thigh.[174] T/NT ratios of 2-2.5 for infected and 1.5-1.8 for inflamed tissues were reported (3 h post injection). Although the differences in uptake between an inflammation and an infection were significant, it was difficult to discriminate between them when evaluating the scintigrams. The authors expanded their approach for imaging infections with other ^{99m}Tc-labeled bacteriophages, such as P22, E79, VD-13 and 60.[175] Moderate to high in vivo T/NT ratios (2.1-14.2) were reported for infections with their target bacteria. However, for all imaging studies with all bacteriophages high liver uptake was observed.

Summary

The strength and at the same time the limitation of bacteriophages is that they only have affinity for specific bacterial strains, which would make it necessary to develop multiple bacteriophages for each bacterial strain of interest. A broad spectrum bacteriophage or a library of bacteriophages directed against multiple bacterial strains would be more widely applicable and would make this class of tracers into a high potential approach.

Quorum-sensing

A very new field of bacterial targeting is the targeting of the cell-to-cell communication amongst bacteria. This communication, via quorum-sensing, is based on the excretion of certain compounds that are recognized by neighboring bacteria via specific extracellular receptors (scheme 1A). The targeting of these receptors is a new approach of labeling bacteria.

Labeling methods

Gomes et al. used the well-known class of gram-negative bacterial quorum-sensing molecules *N*-acyl-L-homoserine lactones (AHLs), which are recognized by the CepR-receptor. L-homoserine lactone was labeled with rhodamine B via an alkyl chain, which resulted in a fluorescent-labeling agent for QS receptors (FLAQS) (**82**).[178]

Bacterial imaging studies

B. cenocepacia is a pathogen that infects mainly patients suffering from cystic fibrosis or with an compromised immunity. This bacterium was successfully labeled by FLAQS in vitro, both in an isolated sample as in a mix of CepR-expressing and CepR-knockout bacteria.[178] No labeling was observed of bacterial strains that do not express the CepR receptor.

Summary

Although a very new field of bacterial imaging, targeting the bacteria via their communication system is a very elegant and promising approach. Each bacterial strain will have their own language (different set of compounds) which can be used as target.

Enzyme activated tracers

The enzymatically activatable tracers are a very interesting class of fluorescent tracers that utilize an approach that is already successfully applied in the field of oncology. These fluorescently silent tracers regain their fluorescence upon cleavage by bacterial proteolytic enzymes (scheme 1A). There are different mechanisms to reversibly silence fluorescent compounds, namely: i) via the presence of a fluorescence-quencher next to the fluorescent moiety, ii) the combination of a FRET pair, or iii) via the inactivation of the fluorescent dye by a reversible disruption of its conjugated system. Several classes of bacterial proteolytic enzymes have been targeted.

β-lactamase activatable tracers

β-lactamases are a class of bacterial enzymes that hydrolyze β-lactams, which are chemical moieties present in e.g. β-lactam antibiotics such as penicillin. Hydrolyzing the β-lactam deactivates the antibiotic and bacteria expressing a β-lactamase are resistant to this class of antibiotics. β-lactamases are not expressed by eukaryotes, but can be introduced as a reporter gene of successful transfection. FRET-pairs separated by a β-lactam moiety were developed as tracers to deliver a visible signal upon successful gene incorporation.[179-181]

Bacterial imaging with β-lactamase-sensitive tracers was introduced by Kong et al. They applied a Cy5.5 dye and a quencher (QSY21-derivative) linked via a β-lactam linker (fig. 7B; **83, 84**). In vitro a 10-fold increase in fluorescence was detected upon cleavage of this linker by β-lactamase. This tracer was able to identify 10^4 viable CFU *M. tuberculosis* in lungs of infected mice via fluorescence imaging (Fig. 7A).[182,183] Infected macrophages could also be analyzed by fluorescence-activated cell sorting (FACS). Response monitoring to antibiotic treatment was also performed and visualized with this tracer, both in vitro and in vivo.[183]

Figure 7.

The fluorescence of a fluorescein derivative (Oregon green 488; **85**) was disrupted by linking two β-lactamase substrates to the core of the dye. Upon cleavage by β-lactamase the fluorescence was restored.[184]

The described β-lactam tracers are generally not considered to be selective for the different β-lactamases. However, Zhang et al recently reported a β-lactam tracer with a fluorescein and rhodamine FRET pair (440-590nm; **86, 87**), which showed different levels of cleavage by several subtypes of β-lactamase.[185]

Protease activation

Bacteria express multiple proteases to cleave signal peptides from newly synthesized proteins, to modify their own biological surroundings for survival, to grow and to defend themselves from attacks by the immune system and other bacteria. In contrast to their mammalian counterparts, certain bacterial proteases are capable of processing D-amino acids. A FRET-based protease sensitive tracer based on D-amino acids was developed for the identification of several bacterial species. Fluorescein and dabcyl were coupled to several peptide sequences containing D-amino acids, which resulted in tracers with selectivity towards a limited number of Bacillus strains including B. anthracis (**88, 89**).[186,187] Because eukaryotic proteases are not able to process D-amino acid residues these tracers are promising candidates for the specific imaging of bacterial infections.

Sortase

Sortase is an enzyme expressed by gram-positive bacteria to conjugate proteins to their extracellular peptidoglycan layer. The presentation of protein factors on the outer leaflet is an important feature of the bacterial virulence and disruption of this conjugation process is considered an alternative for the treatment of infections with drug resistant bacteria.[188] Therefore, identifying the presence and activity of bacterial sortases has intensively been studied. In 2002 Kruger et al. described the synthesis of a potentially interesting tracer containing a FRET pair (rhodamine/fluorescein, 450/585nm; **90**) linked via the peptide sequence -LPETG-, which is cleaved by sortase.[189] Unfortunately, no data of this tracer in action, either in vitro or in vivo, were published.

Other combinations of dyes have been conjugated to the -LPETG- peptide sequence and have been used to screen bacterial samples for the presence of sortases or for the screening of potential sortase inhibitors. Examples are: peptides labeled with 2,4-dinitrophenyl/o-aminobenzoyl (317/420 nm; **91**) and with dabcyl/edans (350/495nm; **92**).[190-194] Infection imaging based on the activity of sortase has not been performed yet.

Pretargeting with sortase

By introducing reactive moieties on gram-positive bacteria by sortase a pretargeting approach was developed. This approach was first tested by direct labeling with fluorescein (**93**), which yielded fluorescently labeled bacteria in vitro.[195] Next, an azide moiety was introduced onto the bacterial peptidoglycan layer via sortase.[195] A secondary labeling could then be performed via a copper-free click reaction with Alexa Fluor 488-DIFO (**94**).

Other activatable compounds

The chromogenic antibacterial compounds based on phenoxazinone have been deactivated by coupling to β-alanine (**95**). The presence of bacterial β-alanylaminopeptidase can reactivate the chromo- or fluorophore yielding a visible signal. A detection based on a chromophore was first attempted and the tracer visualized different species of bacteria based on the colored read-out.[196] A similar approach was conducted using N-aminoacylnaphthyridines (**96**). Upon cleavage of the β-alanyl moiety, fluorescence was detected on agar-plates (350/370-440 nm), however, the obtained signals were too low for in vivo applications.[197]

Staphylococcal strains produce staphylocoagulase, an enzyme that forms a selective protease together with prothrombin and is able to metabolize fibrinogen into fibrin. In this process it cleaves after the sequence X-Val-Pro-Arg-. This enzymatic action has been exploited to develop activatable fluorescent tracers based on coumarin to visualize staphylococcal strains.[198,199] The sensitivity of these probes was improved by making a rhodamine version of these activatable probes (**97**), which has been applied in in vitro screenings.[200]

Summary

Enzyme activatable infection tracers hold great promise and deserve much more attention in our view. Especially the low background signal, until these tracers are activated by bacteria, makes this class of imaging tracers ideal for local and topical applications. The main challenges for the further development of activatable tracers are achieving specificity for bacterial enzymes and generating a strong enough signal to facilitate in vivo imaging.

Proteins

In addition to the above, a number of proteins have also been reported.

The protein-based class of bacterial imaging tracers consists mainly of endogenous proteins that are required by the bacteria, either for their own virulence or as a source of crucial nutrients and growth factors (scheme 1A). These proteins can be converted into imaging tracers by conjugating them with a suitable label. We here only mention the most promising candidate prothrombin; the other candidates are listed in the SI.

Prothrombin

Staphylococcal strains are capable of secreting a fibrinogen-binding protein (staphylocoagulase). Prothrombin binds to staphylocoagulase to form an active complex that has fibrinogen-clotting capabilities, which in turn acts as a virulence factor in the infection pathogenesis.[201] Labeled prothrombin has been used to image S. aureus in endocarditis. The labeling of prothrombin was performed via a small inhibitory peptide that binds covalently in the active site of prothrombin (fig. 8B). Next, a thiol group located in this small inhibitory peptide was deprotected and subsequently labeled with Alexa680-maleimide or ^{64}Cu-DTPA for fluorescence molecular tomography-computed tomography (FMT-CT) or PET-CT imaging, respectively.[202] Coagulase-positive S. aureus bacteria were detected in a mouse endocarditis model by both PET- and FMT-imaging techniques (fig. 8A).

Figure 8.

Summary

The class of protein-based bacterial tracers is quite diverse and their specificity is still under debate. Due to their medium to large molecular size their targeting of infections will most likely be based on both non-specific accumulation and specific targeting.

Discussion

Most tracers we have described in this review were developed with the intention to image bacterial infections. Evidently such tracers hold great medical potential if they: i) lead to clinical detection of infections, ii) enable discrimination between sterile inflammations and bacterial infections, and iii) allow for therapy response monitoring. Although the majority of the bacterial tracers still rely on rather generic targeting moieties, we are under the impression that, similar to e.g. cancer diagnostics, the field of bacterial imaging is moving towards more biomarker specific approaches. This can mean specific targeting of membranous biomarkers or the use of specific enzymatic activation pathways.

A major hurdle in the development of infection specific imaging agents is the selectivity for infections over inflammatory processes. Although the in this review described imaging tracers are developed to target bacteria specifically, many of them could not fulfill that expectation. Since good comparative studies are lacking it is difficult to support one approach over the other. Nevertheless, we defined "potential" in four categories: 1) tracers that are well investigated and where first-in-human data is available, 2) tracers that will be relatively easily introduced in the clinic, 3) promising tracers that utilize a concept proven in other imaging approaches, 4) innovative new concepts.

Three tracers from the well-studied tracer families belong in category 1:

I)   the AMP ^{99m}Tc-UBI$_{29-41}$ (**22b**) has been subject of several clinical studies into the imaging of infections. The obtained imaging data show specificity for bacterial

infections in multiple clinical studies, however the reported T/NT ratios are relatively low.

II)   The nucleoside analog [^{124}I]FIAU (**34**) is entrapped in bacteria after phosphorylation by thymidine kinase.

III)   Antibiotic isoniazid has been conjugated to the chelate DTPA to form a dimeric compound DTPA-bis(INH) (**77**) which has shown great potential in imaging extrapulmonary TB infections.

Imaging tracers based on already clinically applied compounds, which are used for other indications, belong in category 2. Their GMP availability should make their clinical use in bacterial imaging applications more straightforward. In this category a number of antibiotics should be classified: ^{99m}Tc-Vancomycin, ^{99m}Tc-rifampicin, ^{99m}Tc-pheophorbide-a and [^{131}I]linezolid (**38, 71, 72, and 78**). There are, however, some drawbacks of the use of antibiotics for imaging. For example, they are of no value when the invading pathogen is resistant to the used antibiotic and the use of antibiotics at sub-therapeutic dosages may promote the development of resistant bacterial strains.[168]

Enzyme activatable bacterial tracers in our view belong in category 3 and are a promising class of infection specific tracers. Activatable tracers can be used during local (topical) tracer administration, whereby the biggest challenge lies with the reduction of nonspecific background signals: washing away of unbound tracer is not always an option. Uniquely, fluorescent silent compounds can be made fluorescent after activation by bacterial proteases or by binding to bacterial membranes.[203] The concept of enzymatically activatable tracers has already been successfully applied in the field of oncology and the concept will -in our view- also be very well applicable in the field of infection imaging.[204]

Category 4 includes the application of bacteriophages and targeting quorum sensing. These approaches have a high potential through their selectivity for individual classes of bacteria. However more exploratory research is required in these areas.

In this review we have focused on two imaging modalities, being nuclear imaging and fluorescence imaging. Each of these modalities has its own strengths and weaknesses. Nuclear imaging is ideal for detecting hidden and deep seeded infections. Due to its high tissue penetration it allows non-invasive whole body scanning. This said, nuclear imaging has a low spatial resolution and real-time surgical imaging is difficult. Fluorescence imaging has a high spatial resolution and can be visualized in real-time by dedicated fluorescence camera systems, thus allowing for a surgical use.[205,206] Unfortunately, optical imaging suffers from poor tissue penetration, even for dyes in the favorable near infrared window, the tissue penetration is limited to approximately one centimeter.[207] For superficial applications, such as surgical wound infections, prosthetic surface inspections or even with laparoscopic inspections, tissue attenuation is less of a problem. An additional advantage of

fluorescence is that it enables multiplexing;[208] a technique that can simultaneously detect multiple fluorescence emissions e.g. coming from different bacterial strains present in the surgical wound.

We reason that similar to image guided procedures in oncology in the future hybrid approaches, wherein the tracers are both radioactive and fluorescent, may be used for bacterial targeting (scheme 1B).[209,210] A hybrid approach would be very well suited for the identification of deep seeded and hidden bacterial infections. At the same time the fluorescence component of the tracer may be used to provide the surgeon with a visible signal to verify the complete removal of the infection. Furthermore, the fluorescence can still be detected and analyzed at pathology, which can possibly provide additional data about the specific infection and the efficiency of the bacterial targeting.[211]

Conclusions

In the field of imaging bacterial infections interesting developments are ongoing. A number of compounds have been developed that demonstrated a potential value in infection models. Some of these compounds have already been used in the clinic, while other more experimental approaches show great potential. Due to the increasing demand for surgical guidance technology, the field is more and more moving towards embracing fluorescence as imaging modality.

In our opinion the current challenges lie in the identification of new specific targeting mechanisms and further optimization of the bacteria targeting moieties described so far. When more specific bacterial tracers become available for clinical use, such compounds may have a serious impact on global healthcare.

Supporting information
Additional information about proteins applied for bacterial imaging, the chemical structures of the discussed tracers, and tables comparing the imaging performed with these tracers are provided in the supporting information. This material is available free of charge via the internet at http://pubs.acs.org.

Abbreviations:

AMP: antimicrobial peptide

CFU: colony forming units

CT: computed tomography

FACS: fluorescence-activated cell sorting

FMT: fluorescence molecular tomography

FRET: förster resonance energy transfer

iv: intravenous

MRI: magnetic resonance imaging

PET: positron emission tomography

QD: quantum dot

SPECT: single-photon emission computed tomography

T/NT: target to non-target

References

(1)   World Health Organisation, *Global Tuberculosis Control 2010*, **2010,** Geneva.
(2)   Palestro, C.J., Love, C., and Miller, T.T., (2006) Infection and musculoskeletal conditions: Imaging of musculoskeletal infections. *Best Pract. Res. Clin. Rheumatol. 20,* 1197-1218.
(3)   Thigpen, M.C., Whitney, C.G., Messonnier, N.E., Zell, E.R., Lynfield, R., et al., (2011) Bacterial meningitis in the United States, 1998-2007. *New Engl. J. Med. 364,* 2016-2025.
(4)   Gaca, J.G., Sheng, S., Daneshmand, M.A., O'Brien, S., Rankin, J.S., et al., (2011) Outcomes for endocarditis surgery in North America: a simplified risk scoring system. *J. Thorac. Cardiovasc. Surg. 141,* 98-106.
(5)   Health protection agency, *Fifth report of the mandatory surveillance of surgical site infection in orthopaedic surgery*, **2009,** London.
(6)   Walter, C.J., Dumville, J.C., Sharp, C.A., and Page, T., (2012) Systematic review and meta-analysis of wound dressings in the prevention of surgical-site infections in surgical wounds healing by primary intention. *Br. J. Surg. 99,* 1185-1194.
(7)   Rahmim, A. and Zaidi, H., (2008) PET versus SPECT: strengths, limitations and challenges. *Nucl. Med. Commun. 29,* 193-207.
(8)   Buckle, T., van Leeuwen, A.C., Chin, P.T., Janssen, H., Muller, S.H., et al., (2010) A self-assembled multimodal complex for combined pre- and intraoperative imaging of the sentinel lymph node. *Nanotech. 21,* 355101.
(9)   Brouwer, O.R., Klop, W.M.C., Buckle, T., van den Brekel, M.W.M., Balm, A.J.M., et al., (2012) Feasibility of sentinel node biopsy in head and neck melanoma using a hybrid radioactive and fluorescent tracer. *Ann. Surg. Oncol. 19,* 1988-1994.
(10)   Bunschoten, A., Buckle, T., Visser, N., Kuil, J., Yuan, H., et al., (2012) Multimodal interventional molecular imaging of tumor margins and distant metastases by targeting the αvβ3 integrin. *ChemBioChem 13,* 1039-1045.
(11)   Signore, A., Mather, S.J., Piaggio, G., Malviya, G., and Dierckx, R.A., (2010) Molecular imaging of inflammation/infection: nuclear medicine and optical imaging agents and methods. *Chem. Rev. 110,* 3112-3145.
(12)   Dorward, D.A., Lucas, C.D., Rossi, A.G., Haslett, C., and Dhaliwal, K., (2012) Imaging inflammation: Molecular strategies to visualize key components of the inflammatory cascade, from initiation to resolution. *Pharmacol. Ther. 135,* 182-199.
(13)   Lavender, J.P., Lowe, J., Barker, J.R., Burn, J.I., and Chaudhri, M.A., (1971) Gallium 67 citrate scanning in neoplastic and inflammatory lesions. *Br. J. Radiol. 44,* 361-366.
(14)   Tsan, M.F., (1985) Mechanism of Ga-67 Accumulation in Inflammatory Lesions. *J. Nucl. Med. 26,* 88-92.
(15)   Rizzello, A., Di Pierro, D., Lodi, F., Trespidi, S., Cicoria, G., et al., (2009) Synthesis and quality control of 68Ga citrate for routine clinical PET. *Nucl. Med. Commun. 30,* 542-545.
(16)   Nanni, C., Errani, C., Boriani, L., Fantini, L., Ambrosini, V., et al., (2010) 68Ga-citrate PET/CT for evaluating patients with infections of the bone: preliminary results. *J. Nucl. Med. 51,* 1932-1936.
(17)   Kumar, V., Boddeti, D.K., Evans, S.G., and Angelides, S., (2012) (68)Ga-Citrate-PET for diagnostic imaging of infection in rats and for intra-abdominal infection in a patient. *Curr. Radiopharm. 5,* 71-75.
(18)   McAfee, J.G. and Thakur, M.L., (1976) Survey of radioactive agents for in vitro labeling of phagocytic leukocytes. I. Soluble agents. *J. Nucl. Med. 17,* 480-487.
(19)   Peters, A.M., Danpure, H.J., Osman, S., Hawker, R.J., Henderson, B.L., et al., (1986) Clinical experience with 99mTc-hexamethylpropylene-amineoxime for labelling leucocytes and imaging inflammation. *Lancet 2,* 946-949.
(20)   Datz, F.L., (1994) Indium-111-labeled leukocytes for the detection of infection: current status. *Semin. Nucl. Med. 24,* 92-109.
(21)   Forstrom, L.A., Mullan, B.P., Hung, J.C., Lowe, V.J., and Thorson, L.M., (2000) 18F-FDG labelling of human leukocytes. *Nucl. Med. Commun. 21,* 691-694.
(22)   Dumarey, N., Egrise, D., Blocklet, D., Stallenberg, B., Remmelink, M., et al., (2006) Imaging infection with 18F-FDG-labeled leukocyte PET/CT: initial experience in 21 patients. *J. Nucl. Med. 47,* 625-632.

(23)   Dumarey, N., (2009) Imaging with FDG labeled leukocytes: is it clinically useful? *Q. J. Nucl. Med. Mol. Im. 53,* 89-94.

(24)   Bhargava, K.K., Gupta, R.K., Nichols, K.J., and Palestro, C.J., (2009) In vitro human leukocyte labeling with (64)Cu: an intraindividual comparison with (111)In-oxine and (18)F-FDG. *Nucl. Med. Biol. 36,* 545-549.

(25)   Leevy, W.M., Johnson, J.R., Lakshmi, C., Morris, J., Marquez, M., et al., (2006) Selective recognition of bacterial membranes by zinc(II)-coordination complexes. *Chem. Commun.* 1595-1597.

(26)   Leevy, W.M., Gammon, S.T., Jiang, H., Johnson, J.R., Maxwell, D.J., et al., (2006) Optical imaging of bacterial infection in living mice using a fluorescent near-infrared molecular probe. *J. Am. Chem. Soc. 128,* 16476-16477.

(27)   Leevy, W.M., Gammon, S.T., Johnson, J.R., Lampkins, A.J., Jiang, H., et al., (2008) Noninvasive optical imaging of staphylococcus aureus bacterial infection in living mice using a Bis-dipicolylamine-Zinc(II) affinity group conjugated to a near-infrared fluorophore. *Bioconjug. Chem. 19,* 686-692.

(28)   Thakur, M.L., Zhang, K., Paudyal, B., Devakumar, D., Covarrubias, M.Y., et al., (2012) Targeting apoptosis for optical imaging of infection. *Mol. Imaging Biol. 14,* 163-171.

(29)   White, A.G., Gray, B.D., Pak, K.Y., and Smith, B.D., (2012) Deep-red fluorescent imaging probe for bacteria. *Bioorg. Med. Chem. Lett. 22,* 2833-2836.

(30)   DiVittorio, K.M., Leevy, W.M., O'Neil, E.J., Johnson, J.R., Vakulenko, S., et al., (2008) Zinc(II) coordination complexes as membrane-active fluorescent probes and antibiotics. *Chembiochem 9,* 286-293.

(31)   Johnson, J.R., Fu, N., Arunkumar, E., Leevy, W.M., Gammon, S.T., et al., (2007) Squaraine rotaxanes: superior substitutes for Cy-5 in molecular probes for near-infrared fluorescence cell imaging. *Angew. Chem. Int. Ed. Engl. 46,* 5528-5531.

(32)   White, A.G., Fu, N., Leevy, W.M., Lee, J.J., Blasco, M.A., et al., (2010) Optical imaging of bacterial infection in living mice using deep-red fluorescent squaraine rotaxane probes. *Bioconjug. Chem. 21,* 1297-1304.

(33)   Leevy, W.M., Lambert, T.N., Johnson, J.R., Morris, J., and Smith, B.D., (2008) Quantum dot probes for bacteria distinguish Escherichia coli mutants and permit in vivo imaging. *Chem. Commun.* 2331-2333.

(34)   Liu, X., Cheng, D., Gray, B.D., Wang, Y., Akalin, A., et al., (2012) Radiolabeled Zn-DPA as a potential infection imaging agent. *Nucl. Med. Biol. 39,* 709-714.

(35)   Koulov, A.V., Stucker, K.A., Lakshmi, C., Robinson, J.P., and Smith, B.D., (2003) Detection of apoptotic cells using a synthetic fluorescent sensor for membrane surfaces that contain phosphatidylserine. *Cell Death Differ. 10,* 1357-1359.

(36)   Lakshmi, C., Hanshaw, R.G., and Smith, B.D., (2004) Fluorophore-linked zinc(II)dipicolylamine coordination complexes as sensors for phosphatidylserine-containing membranes. *Tetrahedron 60,* 11307-11315.

(37)   Hanshaw, R.G., Lakshmi, C., Lambert, T.N., Johnson, J.R., and Smith, B.D., (2005) Fluorescent detection of apoptotic cells by using zinc coordination complexes with a selective affinity for membrane surfaces enriched with phosphatidylserine. *Chembiochem 6,* 2214-2220.

(38)   Smith, B.A., Xiao, S., Wolter, W., Wheeler, J., Suckow, M.A., et al., (2011) In vivo targeting of cell death using a synthetic fluorescent molecular probe. *Apoptosis 16,* 722-731.

(39)   Smith, B.A., Gammon, S.T., Xiao, S., Wang, W., Chapman, S., et al., (2011) In vivo optical imaging of acute cell death using a near-infrared fluorescent zinc-dipicolylamine probe. *Mol. Pharm. 8,* 583-590.

(40)   Smith, B.A., Harmatys, K.M., Xiao, S., Cole, E.L., Plaunt, A.J., et al., (2013) Enhanced Cell Death Imaging Using Multivalent Zinc(II)-bis(dipicolylamine) Fluorescent Probes. *Mol. Pharm. 10,* 3296-3303.

(41)   Smith, B.A., Akers, W.J., Leevy, W.M., Lampkins, A.J., Xiao, S., et al., (2010) Optical imaging of mammary and prostate tumors in living animals using a synthetic near infrared zinc(II)-dipicolylamine probe for anionic cell surfaces. *J. Am. Chem. Soc. 132,* 67-69.

(42)   Park, C.B., Kim, H.S., and Kim, S.C., (1998) Mechanism of action of the antimicrobial peptide buforin II: buforin II kills microorganisms by penetrating the cell membrane and inhibiting cellular functions. *Biochem. Biophys. Res. Commun. 244,* 253-257.

(43)   Arcidiacono, S., Pivarnik, P., Mello, C.M., and Senecal, A., (2008) Cy5 labeled antimicrobial peptides for enhanced detection of Escherichia coli O157:H7. *Biosens. Bioelectron. 23,* 1721-1727.

(44)   Benincasa, M., Pacor, S., Gennaro, R., and Scocchi, M., (2009) Rapid and reliable detection of antimicrobial peptide penetration into gram-negative bacteria based on fluorescence quenching. *Antimicrob. Agents Chemother. 53,* 3501-3504.

(45)   Benincasa, M., Pelillo, C., Zorzet, S., Garrovo, C., Biffi, S., et al., (2010) The proline-rich peptide Bac7(1-35) reduces mortality from Salmonella typhimurium in a mouse model of infection. *BMC Microbiol. 10,* 178.

(46)   Hasper, H.E., Kramer, N.E., Smith, J.L., Hillman, J.D., Zachariah, C., et al., (2006) An alternative bactericidal mechanism of action for lantibiotic peptides that target lipid II. *Science 313,* 1636-1637.

(47)   Welling, M.M., Nibbering, P.H., Paulusma-Annema, A., Hiemstra, P.S., Pauwels, E.K., et al., (1999) Imaging of bacterial infections with 99mTc-labeled human neutrophil peptide-1. *J. Nucl. Med. 40,* 2073-2080.

(48)   Welling, M.M., Paulusma-Annema, A., Balter, H.S., Pauwels, E.K., and Nibbering, P.H., (2000) Technetium-99m labelled antimicrobial peptides discriminate between bacterial infections and sterile inflammations. *Eur. J. Nucl. Med. 27,* 292-301.

(49)   Brouwer, C.P. and Welling, M.M., (2008) Various routes of administration of (99m)Tc-labeled synthetic lactoferrin antimicrobial peptide hLF 1-11 enables monitoring and effective killing of multidrug-resistant Staphylococcus aureus infections in mice. *Peptides 29,* 1109-1117.

(50)   Liberatore, M., Pala, A., Scaccianoce, S., Anagnostou, C., Di Tondo, U., et al., (2009) Microbial targeting of 99mTc-labeled recombinant human beta-defensin-3 in an animal model of infection: a feasibility pilot study. *J. Nucl. Med. 50,* 823-826.

(51)   Welling, M.M., Brouwer, C.P., van 't Hof, W., Veerman, E.C., and Amerongen, A.V., (2007) Histatin-derived monomeric and dimeric synthetic peptides show strong bactericidal activity towards multidrug-resistant Staphylococcus aureus in vivo. *Antimicrob. Agents Chemother. 51,* 3416-3419.

(52)   Brouwer, C.P., Bogaards, S.J., Wulferink, M., Velders, M.P., and Welling, M.M., (2006) Synthetic peptides derived from human antimicrobial peptide ubiquicidin accumulate at sites of infections and eradicate (multi-drug resistant) Staphylococcus aureus in mice. *Peptides 27,* 2585-2591.

(53)   Visentin, R., Welling, M.M., Tognetto, L., Feitsma, R.I.J., Mazzi, U., et al., (2002) Labelled antimicrobial peptide UBI 29-41: Comparison among 99mTc-UBI, 99mTc-MAG3-UBI, 123I-UBI. *Techn. Rhen. and Other Metals Chem. Nucl. Med. 6,* 695-699.

(54)   Welling, M.M., Visentin, R., Feitsma, H.I., Lupetti, A., Pauwels, E.K., et al., (2004) Infection detection in mice using 99mTc-labeled HYNIC and N2S2 chelate conjugated to the antimicrobial peptide UBI 29-41. *Nucl. Med. Biol. 31,* 503-509.

(55)   Zijlstra, S., Gunawan, J., Freytag, C., and Burchert, W., (2006) Synthesis and evaluation of fluorine-18 labelled compounds for imaging of bacterial infections with pet. *Appl. Rad. Isotopes 64,* 802-807.

(56)   Ebenhan, T., Govender, T., Kruger, G., Pulker, T., Zeevaart, J.R., et al., (2012) Synthesis of 68Ga-NOTA-UBI30-41 and in vivo biodistribution in vervet monkeys towards potential PET/CT imaging of infection. *J. Nucl. Med. 53 S1,* 1520.

(57)   Liu, C. and Gu, Y., (2013) Noninvasive optical imaging of staphylococcus aureus infection in vivo using an antimicrobial peptide fragment based near-infrared fluorescent probes. *J. Innov. Opt. Health Sci. 6,* 1350026.

(58)   Seo, J., Ren, G., Liu, H., Miao, Z., Park, M., et al., (2012) In Vivo Biodistribution and Small Animal PET of (64)Cu-Labeled Antimicrobial Peptoids. *Bioconjug. Chem. 23,* 1069-1079.

(59)   Kuru, E., Hughes, H.V., Brown, P.J., Hall, E., Tekkam, S., et al., (2012) In situ probing of newly synthesized peptidoglycan in live bacteria with fluorescent D-amino acids. *Angew. Chem. Int. Ed. Engl. 51,* 12519-12523.

(60)   Siegrist, M.S., Whiteside, S., Jewett, J.C., Aditham, A., Cava, F., et al., (2013) d-Amino Acid Chemical Reporters Reveal Peptidoglycan Dynamics of an Intracellular Pathogen. *ACS Chem. Biol. 8,* 500-505.

(61)   Welling, M.M., Lupetti, A., Balter, H.S., Lanzzeri, S., Souto, B., et al., (2001) 99mTc-labeled antimicrobial peptides for detection of bacterial and Candida albicans infections. *J. Nucl. Med. 42,* 788-794.

(62)   van Berkel, P.H., Welling, M.M., Geerts, M., van Veen, H.A., Ravensbergen, B., et al., (2002) Large scale production of recombinant human lactoferrin in the milk of transgenic cows. *Nat. Biotechnol. 20,* 484-487.

(63)   Welling, M.M., Mongera, S., Lupetti, A., Balter, H.S., Bonetto, V., et al., (2002) Radiochemical and biological characteristics of 99mTc-UBI 29-41 for imaging of bacterial infections. *Nucl. Med. Biol. 29,* 413-422.

(64)   Ferro-Flores, G., Arteaga de Murphy, C., Pedraza-Lopez, M., Melendez-Alafort, L., Zhang, Y.M., et al., (2003) In vitro and in vivo assessment of 99mTc-UBI specificity for bacteria. *Nucl. Med. Biol. 30,* 597-603.

(65)   Akhtar, M.S., Iqbal, J., Khan, M.A., Irfanullah, J., Jehangir, M., et al., (2004) 99mTc-labeled antimicrobial peptide ubiquicidin (29-41) accumulates less in Escherichia coli infection than in Staphlococcus aureus infection. *J. Nucl. Med. 45,* 849-856.

(66)   Nibbering, P.H., Welling, M.M., Paulusma-Annema, A., Brouwer, C.P., Lupetti, A., et al., (2004) 99mTc-Labeled UBI 29-41 peptide for monitoring the efficacy of antibacterial agents in mice infected with Staphylococcus aureus. *J. Nucl. Med. 45,* 321-326.

(67)   Sarda-Mantel, L., Saleh-Mghir, A., Welling, M.M., Meulemans, A., Vrigneaud, J.M., et al., (2007) Evaluation of 99mTc-UBI 29-41 scintigraphy for specific detection of experimental Staphylococcus aureus prosthetic joint infections. *Eur. J. Nucl. Med. Mol. Im. 34,* 1302-1309.

(68)   Akhtar, M.S., Khan, M.E., Khan, B., Irfanullah, J., Afzal, M.S., et al., (2008) An imaging analysis of (99m)Tc-UBI (29-41) uptake in S. aureus infected thighs of rabbits on ciprofloxacin treatment. *Eur. J. Nucl. Med. Mol. Im. 35,* 1056-1064.

(69)   Brouwer, C.P., Gemmel, F.F., and Welling, M.M., (2010) Evaluation of 99mTc-UBI 29-41 scintigraphy for specific detection of experimental multidrug-resistant Staphylococcus aureus bacterial endocarditis. *Q. J. Nucl. Med. Mol. Im. 54,* 442-450.

(70)   Melendez-Alafort, L., Rodriguez-Cortes, J., Ferro-Flores, G., Arteaga de Murphy, C., Herrera-Rodriguez, R., et al., (2004) Biokinetics of (99m)Tc-UBI 29-41 in humans. *Nucl. Med. Biol. 31,* 373-379.

(71)   Akhtar, M.S., Qaisar, A., Irfanullah, J., Iqbal, J., Khan, B., et al., (2005) Antimicrobial peptide 99mTc-ubiquicidin 29-41 as human infection-imaging agent: clinical trial. *J. Nucl. Med. 46,* 567-573.

(72)   Arteaga de Murphy, C., Gemmel, F., and Balter, J., (2010) Clinical trial of specific imaging of infections. *Nucl. Med. Commun. 31,* 726-733.

(73)   Sepulveda-Mendez, J., Arteaga de Murphy, C., Rojas-Bautista, J.C., and Pedraza-Lopez, M., (2010) Specificity of 99mTc-UBI for detecting infection foci in patients with fever in study. *Nucl. Med. Commun. 31,* 889-895.

(74)   Saeed, S., Zafar, J., Khan, B., Akhtar, A., Qurieshi, S., et al., (2013) Utility of (99)mTc-labelled antimicrobial peptide ubiquicidin (29-41) in the diagnosis of diabetic foot infection. *Eur. J. Nucl. Med. Mol. Im. 40,* 737-743.

(75)   Nazari, B., Azizmohammadi, Z., Rajaei, M., Karami, M., Javadi, H., et al., (2011) Role of 99mTc-ubiquicidin 29-41 scintigraphy to monitor antibiotic therapy in patients with orthopedic infection: a preliminary study. *Nucl. Med. Commun. 32,* 745-751.

(76)   Gandomkar, M., Najafi, R., Shafiei, M., Mazidi, M., Goudarzi, M., et al., (2009) Clinical evaluation of antimicrobial peptide [(99m)Tc/Tricine/HYNIC(0)]ubiquicidin 29-41 as a human-specific infection imaging agent. *Nucl. Med. Biol. 36,* 199-205.
(77)   Ilver, D., Johansson, P., Miller-Podraza, H., Nyholm, P.G., Teneberg, S., et al., (2003) Bacterium-host protein-carbohydrate interactions. *Methods Enzymol. 363,* 134-157.
(78)   Mammen, M., Choi, S., and Whitesides, G.M., (1998) Polyvalent interactions in biological systems: Implications for design and use of multivalent ligands and inhibitors. *Angew. Chem. Int. Ed. Engl. 37,* 2754-2794.
(79)   Disney, M.D., Zheng, J., Swager, T.M., and Seeberger, P.H., (2004) Detection of bacteria with carbohydrate-functionalized fluorescent polymers. *J. Am. Chem. Soc. 126,* 13343-13346.
(80)   Xue, C., Jog, S.P., Murthy, P., and Liu, H., (2006) Synthesis of highly water-soluble fluorescent conjugated glycopoly(p-phenylene)s for lectin and Escherichia coli. *Biomacromolecules 7,* 2470-2474.
(81)   Hirschey, M.D., Han, Y.J., Stucky, G.D., and Butler, A., (2006) Imaging Escherichia coli using functionalized core/shell CdSe/CdS quantum dots. *J. Biol. Inorg. Chem. 11,* 663-669.
(82)   Kloepfer, J.A., Mielke, R.E., Wong, M.S., Nealson, K.H., Stucky, G., et al., (2003) Quantum dots as strain- and metabolism-specific microbiological labels. *Appl. Environ. Microbiol. 69,* 4205-4213.
(83)   Mukhopadhyay, B., Martins, M.B., Karamanska, R., Russell, D.A., and Field, R.A., (2009) Bacterial detection using carbohydrate-functionalised CdS quantum dots: a model study exploiting E. coli recognition of mannosides. *Tet. Lett. 50,* 886-889.
(84)   Backus, K.M., Boshoff, H.I., Barry, C.S., Boutureira, O., Patel, M.K., et al., (2011) Uptake of unnatural trehalose analogs as a reporter for Mycobacterium tuberculosis. *Nat. Chem. Biol. 7,* 228-235.
(85)   Lankinen, P., Lehtimaki, K., Hakanen, A.J., Roivainen, A., and Aro, H.T., (2012) A comparative 18 F-FDG PET/CT imaging of experimantal Staphylococcus aureus osteomyelitis and Staphylococcus epidermidis foreign-bodyassociated infection in the rabbit tibia. *Eur. J. Nucl. Med. Mol. Im. 2,* 41.
(86)   Seshadri, N., Sonoda, L.I., Lever, A.M., and Balan, K., (2012) Superiority of 18F-FDG PET compared to 111In-labelled leucocyte scintigraphy in the evaluation of fever of unknown origin. *J. Infect. 65,* 71-79.
(87)   Parisi, M.T., (2011) Functional imaging of infection: conventional nuclear medicine agents and the expanding role of 18-F-FDG PET. *Pediatr. Radiol. 41,* 803-810.
(88)   Welling, M.M. and Alberto, R., (2010) Performance of a 99mTc-labelled 1-thio-beta-D-glucose 2,3,4,6-tetra-acetate analogue in the detection of infections and tumours in mice: a comparison with [18F]FDG. *Nucl. Med. Commun. 31,* 239-248.
(89)   Martinez, M.E., Kiyono, Y., Noriki, S., Inai, K., Mandap, K.S., et al., (2011) New radiosynthesis of 2-deoxy-2-[(18)F]fluoroacetamido-D-glucopyranose and its evaluation as a bacterial infections imaging agent. *Nucl. Med. Biol. 38,* 807-817.
(90)   Bettegowda, C., Foss, C.A., Cheong, I., Wang, Y., Diaz, L., et al., (2005) Imaging bacterial infections with radiolabeled 1-(2'-deoxy-2'-fluoro-beta-D-arabinofuranosyl)-5-iodouracil. *Proc. Natl. Acad. Sci. U.S.A. 102,* 1145-1150.
(91)   Diaz, L.A., Jr., Foss, C.A., Thornton, K., Nimmagadda, S., Endres, C.J., et al., (2007) Imaging of musculoskeletal bacterial infections by [124I]FIAU-PET/CT. *PLoS One 2,* e1007.
(92)   Pullambhatla, M., Tessier, J., Beck, G., Jedynak, B., Wurthner, J.U., et al., (2012) [125I]FIAU imaging in a preclinical model of lung infection: quantification of bacterial load. *Am. J. Nucl. Med. Mol. Im. 2,* 260-270.
(93)   Jang, S.J., Lee, Y.J., Lim, S., Kim, K.I., Lee, K.C., et al., (2012) Imaging of a localized bacterial infection with endogenous thymidine kinase using radioisotope-labeled nucleosides. *Int. J. Med. Microbiol. 302,* 101-107.
(94)   Ning, X., Lee, S., Wang, Z., Kim, D., Stubblefield, B., et al., (2011) Maltodextrin-based imaging probes detect bacteria in vivo with high sensitivity and specificity. *Nat. Mater. 10,* 602-607.
(95)   Shukla, J., Arora, G., Kotwal, P.P., Kumar, R., Malhotra, A., et al., (2010) Radiolabeled oligosaccharides nanoprobes for infection imaging. *Hell. J. Nucl. Med. 13,* 218-223.
(96)   Dumont, A., Malleron, A., Awwad, M., Dukan, S., and Vauzeilles, B., (2012) Click-Mediated Labeling of Bacterial Membranes through Metabolic Modification of the Lipopolysaccharide Inner Core. *Angew. Chem. Int. Ed. Engl. 51,* 3143-3146.
(97)   Swarts, B.M., Holsclaw, C.M., Jewett, J.C., Alber, M., Fox, D.M., et al., (2012) Probing the Mycobacterial trehalome with bioorthogonal chemistry. *J. Am. Chem. Soc. 134,* 16123-16126.
(98)   Jewett, J.C. and Bertozzi, C.R., (2010) Cu-free click cycloaddition reactions in chemical biology. *Chem. Soc. Rev. 39,* 1272-1279.
(99)   Bakheet, S.M. and Powe, J., (2000) Benign causes of 18-FDG uptake on whole body imaging. *Sem. Nucl. Med. 28,* 352-358.
(100) Treglia, G., Taralli, S., Calcagni, M.L., Maggi, F., Giordano, A., et al., (2011) Is there a role for fluorine 18 fluorodeoxyglucose-positron emission tomography and positron emission tomography/computed tomography in evaluating patients with mycobacteriosis? A systematic review. *J. Comput. Assist. Tomogr. 35,* 387-393.
(101) Ren, W., Muzik, O., Jackson, N., Khoury, B., Shi, T., et al., (2012) Differentiation of septic and aseptic loosening by PET with both 11C-PK11195 and 18F-FDG in rat models. *Nucl. Med. Commun. 33,* 747-756.
(102) Peterson, K.L., Reid, W.C., Freeman, A.F., Holland, S.M., Pettigrew, R.I., et al., (2013) The use of (14)C-FIAU to predict bacterial thymidine kinase presence: Implications for radiolabeled FIAU bacterial imaging. *Nucl. Med. Biol. 40,* 638-642.

(103) Been, L.B., Suurmeijer, A.J., Cobben, D.C., Jager, P.L., Hoekstra, H.J., et al., (2004) [18F]FLT-PET in oncology: current status and opportunities. *Eur. J. Nucl. Med. Mol. Im. 31,* 1659-1672.

(104) Tiyanont, K., Doan, T., Lazarus, M.B., Fang, X., Rudner, D.Z., et al., (2006) Imaging peptidoglycan biosynthesis in Bacillus subtilis with fluorescent antibiotics. *Proc. Natl. Acad. Sci. U.S.A. 103,* 11033-11038.

(105) Pereira, P.M., Filipe, S.R., Tomasz, A., and Pinho, M.G., (2007) Fluorescence ratio imaging microscopy shows decreased access of vancomycin to cell wall synthetic sites in vancomycin-resistant Staphylococcus aureus. *Antimicrob. Agents Chemother. 51,* 3627-3633.

(106) Lunde, C.S., Rexer, C.H., Hartouni, S.R., Axt, S., and Benton, B.M., (2010) Fluorescence microscopy demonstrates enhanced targeting of telavancin to the division septum of Staphylococcus aureus. *Antimicrob. Agents Chemother. 54,* 2198-2200.

(107) Kao, J.C., Geroski, D.H., and Edelhauser, H.F., (2005) Transscleral permeability of fluorescent-labeled antibiotics. *J. Ocul. Pharmacol. Ther. 21,* 1-10.

(108) Dhanapal, R., Perumal, P.T., Damodiran, M., Ramprasath, C., and Mathivanan, N., (2012) Synthesis of quinoline derivatives for fluorescent imaging certain bacteria. *Bioorg. Med. Chem. Lett. 22,* 6494-6497.

(109) Fischman, A.J., Livni, E., Babich, J., Alpert, N.M., Liu, Y.Y., et al., (1992) Pharmacokinetics of 18F-labeled fleroxacin in rabbits with Escherichia coli infections, studied with positron emission tomography. *Antimicrob. Agents Chemother. 36,* 2286-2292.

(110) Livni, E., Babich, J., Alpert, N.M., Liu, Y.Y., Thom, E., et al., (1993) Synthesis and biodistribution of 18F-labeled fleroxacin. *Nucl. Med. Biol. 20,* 81-87.

(111) Tewson, T.J., Yang, D., Wong, G., Macy, D., DeJesus, O.J., et al., (1996) The synthesis of fluorine-18 lomefloxacin and its preliminary use in human studies. *Nucl. Med. Biol. 23,* 767-772.

(112) Motaleb, M.A., (2007) Preparation and biodistribution of 99mTc-lomefloxacin and 99mTc-ofloxacin complexes. *J. Radioanal. Nucl. Chem. 272,* 95-99.

(113) Babich, J.W., Rubin, R.H., Graham, W.A., Wilkinson, R.A., Vincent, J., et al., (1996) 18F-labeling and biodistribution of the novel fluoro-quinolone antimicrobial agent, trovafloxacin (CP 99,219). *Nucl. Med. Biol. 23,* 995-998.

(114) Fischman, A.J., Babich, J.W., Bonab, A.A., Alpert, N.M., Vincent, J., et al., (1998) Pharmacokinetics of [18F]trovafloxacin in healthy human subjects studied with positron emission tomography. *Antimicrob. Agents Chemother. 42,* 2048-2054.

(115) Singh, A.K., Verma, J., Bhatnagar, A., and Ali, A., (2003) Tc-99m labeled sparfloxacin: A specific infection imaging agent. *World J. Nucl. Med. 2,* 103-109.

(116) Siaens, R.H., Rennen, H.J., Boerman, O.C., Dierckx, R., and Slegers, G., (2004) Synthesis and comparison of 99mTc-enrofloxacin and 99mTc-ciprofloxacin. *J. Nucl. Med. 45,* 2088-2094.

(117) El-Ghany, E.A., El-Kolaly, M.T., Amine, A.M., El-Sayed, A.S., and Abdel-Gelil, G., (2005) Synthesis of 99mTc-pefloxacin: A new targeting agent for infectious foci. *J. Radioanal. Nucl. Chem. 266,* 131-139.

(118) El-Ghany, E.A., Amine, A.M., El-Kawy, O.A., and Amin, M., (2007) Technetium-99m labeling and freeze-dried kit formulation of levofloxacin (L-Flox): A novel agent for detecting sites of infection. *J. Label. Compd. Radiopharm. 50,* 25-31.

(119) Qaiser, S.S., Khan, A.U., and Khan, M.R., (2010) Synthesis, biodistribution and evaluation of 99mTc-sitafloxacin kit: a novel infection imaging agent. *J. Radioanal. Nucl. Chem. 284,* 189-193.

(120) Shah, S.Q. and Khan, M.R., (2011) Radiosynthesis and biological evaluation of the (99m)Tc-tricarbonyl moxifloxacin dithiocarbamate complex as a potential Staphylococcus aureus infection radiotracer. *Appl. Rad. Isotopes 69,* 686-690.

(121) Ibrahim, I.T., Motaleb, M.A., and Attalah, K.M., (2010) Synthesis and biological distribution of Tc-99m-norfloxacin complex, a novel agent for detecting sites of infection. *J. Radioanal. Nucl. Chem. 285,* 431-436.

(122) Zhang, S., Zhang, W., Wang, Y., Jin, Z., Wang, X., et al., (2011) Synthesis and biodistribution of a novel (99m)TcN complex of norfloxacin dithiocarbamate as a potential agent for bacterial infection imaging. *Bioconjug. Chem. 22,* 369-375.

(123) Shah, S.Q. and Khan, M.R., (2011) Synthesis of technetium-99m labeled clinafloxacin (99mTc-CNN) complex and biological evaluation as a potential Staphylococcus aureus infection imaging agent. *J. Radioanal. Nucl. Chem. 288,* 423-428.

(124) Motaleb, M.A., (2010) Radiochemical and biological characteristics of 99mTc-difloxacin and 99mTc-pefloxacin for detecting sites of infection. *J. Label. Compd. Radiopharm. 53,* 104-109.

(125) Barreto, G.V., Iglesias, F., Roca, M., Tubau, F., and Martin-Comin, J., (2000) Labelling of ceftizoxime with 99mTc. *Rev. Esp. Med. Nucl. 19,* 479-483.

(126) Diniz, S.O., Rezende, C.M., Serakides, R., Ferreira, R.L., Ribeiro, T.G., et al., (2008) Scintigraphic imaging using technetium-99m-labeled ceftizoxime in an experimental model of acute osteomyelitis in rats. *Nucl. Med. Commun. 29,* 830-836.

(127) Motaleb, M.A., (2007) Preparation of 99mTc-cefoperazone complex, a novel agent for detecting sites of infection. *J. Radioanal. Nucl. Chem. 272,* 167-171.

(128) Lambrecht, F.Y., Durkan, K., and Unak, P., (2007) Preparation, quality control and stability of 99mTc-cefuroxime axetil. *J. Radioanal. Nucl. Chem. 275,* 161-164.

(129) Lambrecht, F.Y., Yilmaz, O., Unak, P., Seyitoglu, B., Durkan, K., et al., (2008) Evaluation of 99mTc-Cefuroxime axetil for imaging of inflammation. *J. Radioanal. Nucl. Chem. 277,* 491-494.

(130) Chattopadhyay, S., Ghosh, M., Sett, S., Das, M.K., Chandra, S., et al., (2012) Preparation and evaluation of 99mTc-cefuroxime, a potential infection specific imaging agent: a reliable thin layer chromatographic system to delineate impurities from the 99mTc-antibiotic. *Appl. Rad. Isotopes 70,* 2384-2387.

(131) Motaleb, M.A., El-Kolaly, M.T., Ibrahim, A.B., and Abd El-Bary, A., (2011) Study on the preparation and biological evaluation of 99mTc-gatifloxacin and 99mTc-cefepime complex. *J. Radioanal. Nucl. Chem. 289,* 57-65.

(132) Mostafa, M., Motaleb, M.A., and Sakr, T.M., (2010) Labeling of ceftriaxone for infective inflammation imaging using 99mTc eluted from 99Mo/99mTc generator based on zirconium molybdate. *Appl. Rad. Isotopes 68,* 1959-1963.

(133) Kaul, A., Hazari, P.P., Rawat, H., Singh, B., Kalawat, T.C., et al., (2012) Preliminary evaluation of technetium-99m-labeled ceftriaxone: infection imaging agent for the clinical diagnosis of orthopedic infection. *Int. J. Infect. Dis. 17,* e263-e270.

(134) Ercan, M.T., Aras, T., and Unsal, I.S., (1992) Evaluation of 99mTc-erythromycin and 99mTc-streptomycin sulphate for the visualization of inflammatory lesions. *Int. J. Rad. Appl. Instrum. B 19,* 803-806.

(135) Roohi, S., Mushtaq, A., Jehangir, M., and Malik, S.A., (2006) Synthesis, quality control and biodistribution of 99mTc-Kanamycin. *J. Radioanal. Nucl. Chem. 267,* 561-566.

(136) Tsopelas, C., Penglis, S., Ruszkiewicz, A., and Bartholomeusz, F.D., (2003) 99mTc-alafosfalin: an antibiotic peptide infection imaging agent. *Nucl. Med. Biol. 30,* 169-175.

(137) Shah, S.Q., Khan, A.U., and Khan, M.R., (2010) Radiosynthesis and biodistribution of (99m)Tc-rifampicin: a novel radiotracer for in-vivo infection imaging. *Appl. Rad. Isotopes 68,* 2255-2260.

(138) Ocakoglu, K., Bayrak, E., Onursal, M., Yilmaz, O., Lambrecht, F.Y., et al., (2011) Evaluation of 99mTc-Pheophorbide-a use in infection imaging: a rat model. *Appl. Rad. Isotopes 69,* 1165-1168.

(139) Halder, K.K., Nayak, D.K., Baishya, R., Sarkar, B.R., Sinha, S., et al., (2011) (99m)Tc-labeling of ciprofloxacin and nitrofuryl thiosemicarbazone using fac-[(99m)Tc(CO)3(H2O)3] core: evaluation of their efficacy as infection imaging agents. *Metallomics 3,* 1041-1048.

(140) Shah, S.Q., Khan, A.U., and Khan, M.R., (2011) Radiosynthesis of 99mTc-nitrofurantoin a novel radiotracer for in vivo imaging of Escherichia coli infection. *J. Radioanal. Nucl. Chem. 287,* 417-422.

(141) Asikoglu, M., Yurt, F., Cagliyan, O., Unak, P., and Ozkilic, H., (2000) Detecting inflammation with 131I-labeled ornidazole. *Appl. Radiat. Isot. 53,* 411-413.

(142) Rossouw, D.D., Lotter, M.G., du Raan, H., Jansen, S.E., Hohn, A., et al., (2005) Radiosynthesis and evaluation of two novel 123I-labeled 2-methyl-4-nitroimidazole derivatives as potential infection imaging agents. *Nucl. Med. Biol. 32,* 385-394.

(143) Lambrecht, F.Y., Yilmaz, O., Durkan, K., Unak, P., and Bayrak, E., (2009) Preparation and biodistribution of [131I]linezolid in animal model infection and inflammation. *J. Radioanal. Nucl. Chem. 281,* 415-419.

(144) Essouissi, I., Ghali, W., Saied, N.M., and Saidi, M., (2010) Synthesis and evaluation of 99mTc-N-sulfanilamide ferrocene carboxamide as bacterial infections detector. *Nucl. Med. Biol. 37,* 821-829.

(145) Singh, A.K., Verma, J., Bhatnagar, A., Sen, S., and Bose, M., (2003) Tc-99m Isoniazid: A specific agent for diagnosis of tuberculosis. *World J. Nucl. Med. 2,* 292-305.

(146) Hazari, P.P., Chuttani, K., Kumar, N., Mathur, R., Sharma, R., et al., (2009) Synthesis and biological evaluation of isonicotinic acid hydrazide conjugated with diethyelenetriaminepentaacetic acid for infection imaging. *Open Nucl. Med. J. 1,* 33-42.

(147) Perkins, H.R. and Nieto, M., (1970) The preparation of iodinated vancomycin and its distribution in bacteria treated with the antibiotic. *Biochem. J. 116,* 83-92.

(148) Roohi, S., Mushtaq, A., and Malik, S.A., (2005) Synthesis and biodistribution of 99mTc-Vancomycin in a model of bacterial infection. *Radiochim. Acta 93,* 415-418.

(149) Jalilian, A.R., Hosseini, M.A., Karimian, A., Saddadi, F., and Sadeghi, M., (2006) Preparation and biodistribution of [201TI](III)vancomycin complex in normal rats. *Nukleonika 51,* 203-208.

(150) Jalilian, A.R., Hosseini, M.A., Majdabadi, A., and Saddadi, F., (2008) Evaluation of [(201)Tl](III) Vancomycin in normal rats. *Nucl. Med. Rev. Cent. East. Eur. 11,* 1-4.

(151) Chung, H.J., Reiner, T., Budin, G., Min, C., Liong, M., et al., (2011) Ubiquitous detection of gram-positive bacteria with bioorthogonal magnetofluorescent nanoparticles. *ACS Nano 5,* 8834-8841.

(152) Solanki, K.K., Bomanji, J., Siraj, Q., Small, M., and Britton, K.E., (1993) 99mTc-infecton: A new class of radiopharmaceutical for imaging infection. *J. Nucl. Med. 34,* 119P.

(153) Vinjamuri, S., Hall, A.V., Solanki, K.K., Bomanji, J., Siraj, Q., et al., (1996) Comparison of 99mTc infecton imaging with radiolabelled white-cell imaging in the evaluation of bacterial infection. *Lancet 347,* 233-235.

(154) Britton, K.E., Wareham, D.W., Das, S.S., Solanki, K.K., Amaral, H., et al., (2002) Imaging bacterial infection with (99m)Tc-ciprofloxacin (Infecton). *J. Clin. Pathol. 55,* 817-823.

(155) Britton, K.E., Vinjamuri, S., Hall, A.V., Solanki, K., Siraj, Q.H., et al., (1997) Clinical evaluation of technetium-99m infecton for the localisation of bacterial infection. *Eur. J. Nucl. Med. 24,* 553-556.

(156) Hall, A.V., Solanki, K.K., Vinjamuri, S., Britton, K.E., and Das, S.S., (1998) Evaluation of the efficacy of 99mTc-Infecton, a novel agent for detecting sites of infection. *J. Clin. Pathol. 51,* 215-219.

(157) Malamitsi, J., Giamarellou, H., Kanellakopoulou, K., Dounis, E., Grecka, V., et al., (2003) Infecton: a 99mTc-ciprofloxacin radiopharmaceutical for the detection of bone infection. *Clin. Microbiol. Infect. 9,* 101-109.

(158) Choe, Y.M., Choe, W., Lee, K.Y., Ahn, S.I., Kim, K., et al., (2007) Tc-99m ciprofloxacin imaging in acute cholecystitis. *World J. Gastroenterol. 13,* 3249-3252.

(159) Sarda, L., Saleh-Mghir, A., Peker, C., Meulemans, A., Cremieux, A.C., et al., (2002) Evaluation of (99m)Tc-ciprofloxacin scintigraphy in a rabbit model of Staphylococcus aureus prosthetic joint infection. *J. Nucl. Med. 43,* 239-245.

(160) Sarda, L., Cremieux, A.C., Lebellec, Y., Meulemans, A., Lebtahi, R., et al., (2003) Inability of 99mTc-ciprofloxacin scintigraphy to discriminate between septic and sterile osteoarticular diseases. *J. Nucl. Med. 44,* 920-926.

(161) Sharma, R., Tewari, K.N., Bhatnagar, A., Mondal, A., Mishra, A.K., et al., (2007) Tc-99m ciprofloxacin scans for detection of tubercular bone infection. *Clin. Nucl. Med. 32,* 367-370.

(162) Palestro, C.J., Love, C., Caprioli, R., Marwin, S., Richardson, H., et al., (2006) Phase II study of 99mTc-ciprofloxacin uptake in patients with high suspicion of osteomyelitis. *J. Nucl. Med. 47, sup 1,* 152P.

(163) Langer, O., Mitterhauser, M., Brunner, M., Zeitlinger, M., Wadsak, W., et al., (2003) Synthesis of fluorine-18-labeled ciprofloxacin for PET studies in humans. *Nucl. Med. Biol. 30,* 285-291.

(164) Langer, O., Brunner, M., Zeitlinger, M., Ziegler, S., Muller, U., et al., (2005) In vitro and in vivo evaluation of [18F]ciprofloxacin for the imaging of bacterial infections with PET. *Eur. J. Nucl. Med. Mol. Im. 32,* 143-150.

(165) Sachin, K., Kim, E.M., Cheong, S.J., Jeong, H.J., Lim, S.T., et al., (2010) Synthesis of N'-[(18)F]fluoroalkylated ciprofloxacin as a potential bacterial infection imaging agent for PET study. *Bioconjug. Chem. 21,* 2282-2288.

(166) Zhang, J., Guo, H., Zhang, S., Lin, Y., and Wang, X., (2008) Synthesis and biodistribution of a novel (99m)TcN complex of ciprofloxacin dithiocarbamate as a potential agent for infection imaging. *Bioorg. Med. Chem. Lett. 18,* 5168-5170.

(167) Dahiya, S., Chuttani, K., Khar, R.K., Saluja, D., Mishra, A.K., et al., (2009) Synthesis and evaluation of Ciprofloxacin derivatives as diagnostic tools for bacterial infection by Staphylococcus aureus. *Metallomics 1,* 409-417.

(168) Kohanski, M.A., DePristo, M.A., and Collins, J.J., (2010) Sublethal antibiotic treatment leads to multidrug resistance via radical-induced mutagenesis. *Mol. Cell 37,* 311-320.

(169) Namura, M., Hijikata, T., Miyanaga, K., and Tanji, Y., (2008) Detection of Escherichia coli with fluorescent labeled phages that have a broad host range to E. coli in sewage water. *Biotechnol. Prog. 24,* 481-486.

(170) Oda, M., Morita, M., Unno, H., and Tanji, Y., (2004) Rapid detection of Escherichia coli O157:H7 by using green fluorescent protein-labeled PP01 bacteriophage. *Appl. Environ. Microbiol. 70,* 527-534.

(171) Mosier-Boss, P.A., Lieberman, S.H., Andrews, J.M., Rohwer, F.L., Wegley, L.E., et al., (2003) Use of fluorescently labeled phage in the detection and identification of bacterial species. *Appl. Spectrosc. 57,* 1138-1144.

(172) Lee, S.H., Onuki, M., Satoh, H., and Mino, T., (2006) Isolation, characterization of bacteriophages specific to Microlunatus phosphovorus and their application for rapid host detection. *Lett. Appl. Microbiol. 42,* 259-264.

(173) Goodridge, L., Chen, J., and Griffiths, M., (1999) The use of a fluorescent bacteriophage assay for detection of Escherichia coli O157:H7 in inoculated ground beef and raw milk. *Int. J. Food Microbiol. 47,* 43-50.

(174) Rusckowski, M., Gupta, S., Liu, G., Dou, S., and Hnatowich, D.J., (2004) Investigations of a (99m)Tc-labeled bacteriophage as a potential infection-specific imaging agent. *J. Nucl. Med. 45,* 1201-1208.

(175) Rusckowski, M., Gupta, S., Liu, G., Dou, S., and Hnatowich, D.J., (2008) Investigation of four (99m)Tc-labeled bacteriophages for infection-specific imaging. *Nucl. Med. Biol. 35,* 433-440.

(176) Wu, L., Huang, T., Yang, L., Pan, J., Zhu, S., et al., (2011) Sensitive and selective bacterial detection using tetracysteine-tagged phages in conjunction with biarsenical dye. *Angew. Chem. Int. Ed. Engl. 50,* 5873-5877.

(177) Edgar, R., McKinstry, M., Hwang, J., Oppenheim, A.B., Fekete, R.A., et al., (2006) High-sensitivity bacterial detection using biotin-tagged phage and quantum-dot nanocomplexes. *Proc. Natl. Acad. Sci. U.S.A. 103,* 4841-4845.

(178) Gomes, J., Huber, N., Grunau, A., Eberl, L., and Gademann, K., (2013) Fluorescent Labeling Agents for Quorum-Sensing Receptors (FLAQS) in Live Cells. *Chemistry 19,* 9766-9770.

(179) Zlokarnik, G., Negulescu, P.A., Knapp, T.E., Mere, L., Burres, N., et al., (1998) Quantitation of transcription and clonal selection of single living cells with beta-lactamase as reporter. *Science 279,* 84-88.

(180) Gao, W., Xing, B., Tsien, R.Y., and Rao, J., (2003) Novel fluorogenic substrates for imaging beta-lactamase gene expression. *J. Am. Chem. Soc. 125,* 11146-11147.

(181) Xing, B., Khanamiryan, A., and Rao, J., (2005) Cell-permeable near-infrared fluorogenic substrates for imaging beta-lactamase activity. *J. Am. Chem. Soc. 127,* 4158-4159.

(182) Kong, Y., Yao, H., Ren, H., Subbian, S., Cirillo, S.L., et al., (2010) Imaging tuberculosis with endogenous beta-lactamase reporter enzyme fluorescence in live mice. *Proc. Natl. Acad. Sci. U.S.A. 107,* 12239-12244.

(183) Kong, Y. and Cirillo, J.D., (2010) Reporter enzyme fluorescence (REF) imaging and quantification of tuberculosis in live animals. *Virulence 1,* 558-562.

(184) Rukavishnikov, A., Gee, K.R., Johnson, I., and Corry, S., (2011) Fluorogenic cephalosporin substrates for beta-lactamase TEM-1. *Anal. Biochem. 419,* 9-16.

(185) Zhang, J., Shen, Y., May, S.L., Nelson, D.C., and Li, S., (2012) Ratiometric fluorescence detection of pathogenic bacteria resistant to broad-spectrum b-lactam antibiotics. *Angew. Chem. Int. Ed. Engl. 51,* 1865-1868.

(186) Kaman, W.E., Hulst, A.G., van Alphen, P.T., Roffel, S., van der Schans, M.J., et al., (2011) Peptide-based fluorescence resonance energy transfer protease substrates for the detection and diagnosis of Bacillus species. *Anal. Chem. 83,* 2511-2517.

(187) Kaman, W.E., Galassi, F., de Soet, J.J., Bizzarro, S., Loos, B.G., et al., (2012) Highly Specific Protease-Based Approach for Detection of Porphyromonas gingivalis in Diagnosis of Periodontitis. *J. Clin. Microbiol. 50,* 104-112.

(188)	Shah, S.Q., Khan, A.U., and Khan, M.R., (2011) (99m)Tc-prulifloxacin in artificially infected animals. Radiosynthesis and biological evaluation. *Nuklearmedizin. Nuclear medicine 50,* 134-140.

(189)	Kruger, R.G., Dostal, P., and McCafferty, D.G., (2002) An economical and preparative orthogonal solid phase synthesis of fluorescein and rhodamine derivatized peptides: FRET substrates for the Staphylococcus aureus sortase SrtA transpeptidase reaction. *Chem. Commun.* 2092-2093.

(190)	Ton-That, H., Mazmanian, S.K., Faull, K.F., and Schneewind, O., (2000) Anchoring of surface proteins to the cell wall of Staphylococcus aureus. Sortase catalyzed in vitro transpeptidation reaction using LPXTG peptide and NH(2)-Gly(3) substrates. *J. Biol. Chem. 275,* 9876-9881.

(191)	Ilangovan, U., Ton-That, H., Iwahara, J., Schneewind, O., and Clubb, R.T., (2001) Structure of sortase, the transpeptidase that anchors proteins to the cell wall of Staphylococcus aureus. *Proc. Natl. Acad. Sci. U.S.A. 98,* 6056-6061.

(192)	Kruger, R.G., Dostal, P., and McCafferty, D.G., (2004) Development of a high-performance liquid chromatography assay and revision of kinetic parameters for the Staphylococcus aureus sortase transpeptidase SrtA. *Anal. Biochem. 326,* 42-48.

(193)	Kruger, R.G., Barkallah, S., Frankel, B.A., and McCafferty, D.G., (2004) Inhibition of the Staphylococcus aureus sortase transpeptidase SrtA by phosphinic peptidomimetics. *Bioorg. Med. Chem. 12,* 3723-3729.

(194)	Chenna, B.C., Shinkre, B.A., King, J.R., Lucius, A.L., Narayana, S.V., et al., (2008) Identification of novel inhibitors of bacterial surface enzyme Staphylococcus aureus Sortase A. *Bioorg. Med. Chem. Lett. 18,* 380-385.

(195)	Nelson, J.W., Chamessian, A.G., McEnaney, P.J., Murelli, R.P., Kazmierczak, B.I., et al., (2010) A biosynthetic strategy for re-engineering the Staphylococcus aureus cell wall with non-native small molecules. *ACS Chem. Biol. 5,* 1147-1155.

(196)	Zaytsev, A.V., Anderson, R.J., Bedernjak, A., Groundwater, P.W., Huang, Y., et al., (2008) Synthesis and testing of chromogenic phenoxazinone substrates for beta-alanyl aminopeptidase. *Org. Biomol. Chem. 6,* 682-692.

(197)	Varadi, L., Gray, M., Groundwater, P.W., Hall, A.J., James, A.L., et al., (2012) Synthesis and evaluation of fluorogenic 2-amino-1,8-naphthyridine derivatives for the detection of bacteria. *Org. Biomol. Chem. 10,* 2578-2589.

(198)	Morita, T., Kato, H., Iwanaga, S., Takada, K., and Kimura, T., (1977) New fluorogenic substrates for alpha-thrombin, factor Xa, kallikreins, and urokinase. *J. Biochem. 82,* 1495-1498.

(199)	Holliday, M.G., Ford, M., Perry, J.D., and Gould, F.K., (1999) Rapid identification of Staphylococcus aureus by using fluorescent staphylocoagulase assays. *J. Clin. Microbiol. 37,* 1190-1192.

(200)	Sinclair, A., Mulcahy, L.E., Geldeard, L., Malik, S., Fielder, M.D., et al., (2013) Development of an in situ culture-free screening test for the rapid detection of Staphylococcus aureus within healthcare environments. *Org. Biomol. Chem. 11,* 3307-3313.

(201)	Smith, W., Hale, J.H., and Smith, M.M., (1947) The role of coagulase in staphylococcal infections. *Br. J. Exp. Pathol. 28,* 57-67.

(202)	Panizzi, P., Nahrendorf, M., Figueiredo, J.L., Panizzi, J., Marinelli, B., et al., (2011) In vivo detection of Staphylococcus aureus endocarditis by targeting pathogen-specific prothrombin activation. *Nat. Med. 17,* 1142-1146.

(203)	Lee, S., Park, K., Kim, K., Choi, K., and Kwon, I.C., (2008) Activatable imaging probes with amplified fluorescent signals. *Chem. Commun.* 4250-4260.

(204)	Urano, Y., Sakabe, M., Kosaka, N., Ogawa, M., Mitsunaga, M., et al., (2011) Rapid Cancer Detection by Topically Spraying a gamma-Glutamyltranspeptidase-Activated Fluorescent Probe. *Sci Transl Med 3,* 1-10.

(205)	Troyan, S.L., Kianzad, V., Gibbs-Strauss, S.L., Gioux, S., Matsui, A., et al., (2009) The FLARE intraoperative near-infrared fluorescence imaging system: a first-in-human clinical trial in breast cancer sentinel lymph node mapping. *Ann. Surg. Oncol. 16,* 2943-2952.

(206)	Themelis, G., Yoo, J.S., Soh, K.S., Schulz, R., and Ntziachristos, V., (2009) Real-time intraoperative fluorescence imaging system using light-absorption correction. *J. Biomed. Opt. 14,* 064012.

(207)	Chin, P.T.K., Beekman, C.A.C., Buckle, T., Josephson, L., and van Leeuwen, F.W.B., (2012) Multispectral visualization of surgical safety-margins using fluorescent marker seeds. *Am. J. Nucl. Med. Mol. Im. 2,* 151-162.

(208)	Evans, R.G., Naidu, B., Rajpoot, N.M., Epstein, D., and Khan, M., (2012) Toponome imaging system: multiplex biomarkers in oncology. *Trends Mol. Med. 18,* 723-731.

(209)	Chin, P.T.K., Welling, M.M., Meskers, S.C., Valdes Olmos, R.A., Tanke, H., et al., (2013) Optical imaging as an expansion of nuclear medicine: Cerenkov-based luminescence vs fluorescence-based luminescence. *Eur. J. Nucl. Med. Mol. Imaging 40,* 1283-1291.

(210)	Van den Berg, N.S., Valdes Olmos, R.A., Van der Poel, H.G., and van leeuwen, F.W.B., (2013) Sentinel lymph node biopsy for prostate cancer: a hybrid approach. *J. Nucl. Med. 54,* 493-496.

(211)	Buckle, T., Kuil, J., Van den Berg, N.S., Bunschoten, A., Lamb, H.J., et al., (2013) Use of a single hybrid imaging agent for integration of target validation with in vivo and ex vivo imaging of mouse tumor lesions resembling human DCIS. *PLoS One 8,* e48324.

(212)	Welling, M.M., Ferro-Flores, G., Pirmettis, I., and Brouwer, C.P.J.M., (2009) Current status of imaging infections with radiolabeled anti-infective agents. *Anti-Infect. Agents Med. Chem. 8,* 272-287.
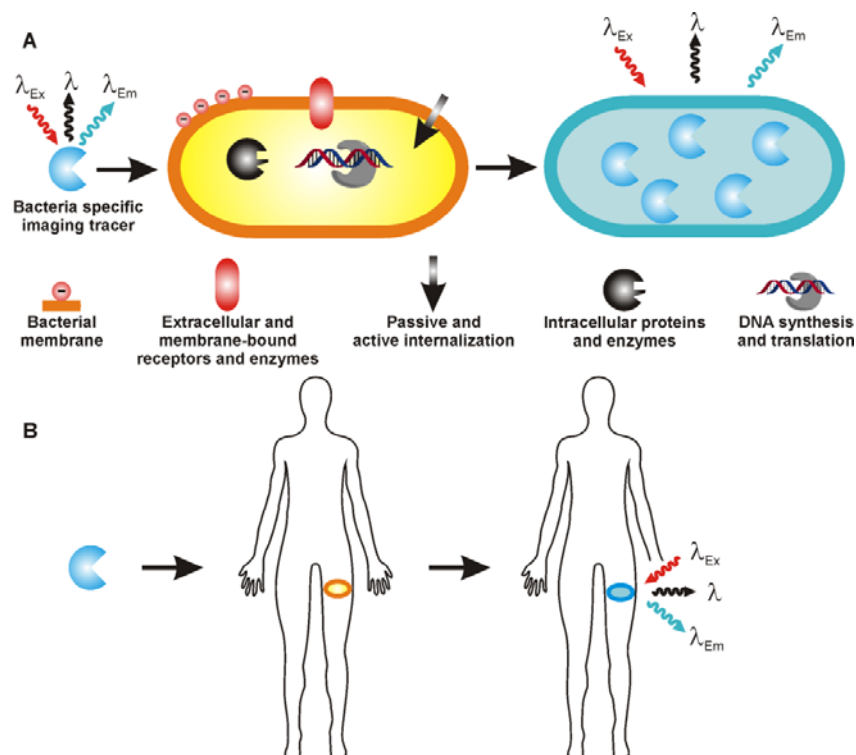
Scheme 1. A) Pathways of bacterial targeting with imaging tracers, B) Bacterial specific imaging tracers, containing a fluorescent, nuclear or hybrid label, can have their applications in locating and diagnosing local and hidden bacterial infections.
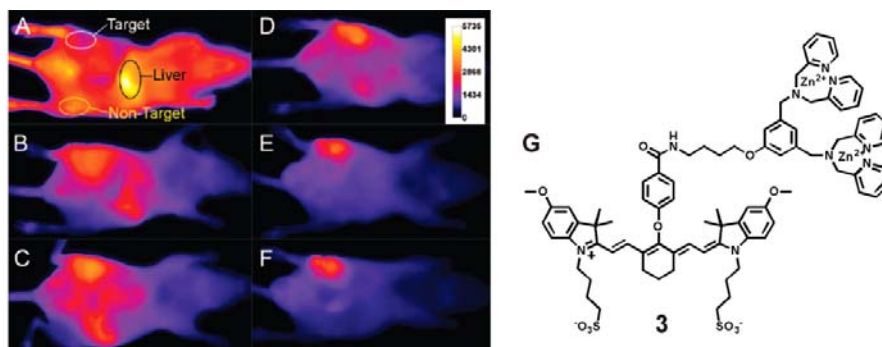

Figure 1. Fluorescence images of S. aureus infected mice. Image taken 0 h (A), 3 h (B), 6 h (C), 12 h (D), 18 h (E), and 21 h (F) after injection of 75 µL of a 1 mM solution of PSVue 794 (**3**) (G). (Reprinted with permission from Matthew et al. Bioconjug. Chem. 2008, 19(3), 686-692. Copyright 2008 American Chemical Society)
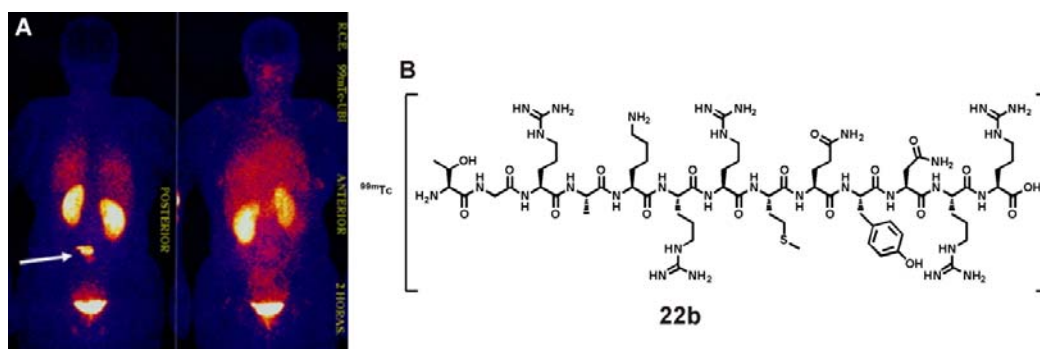
Figure 2. Posterior and anterior view of a patient with a septic process in the lumbar vertebra. The patient was injected with ^{99m}Tc-UBI$_{29-41}$ (**22b**) and imaged by scintigraphy 2 h post injection. (image reproduced from Welling et al.).[212]
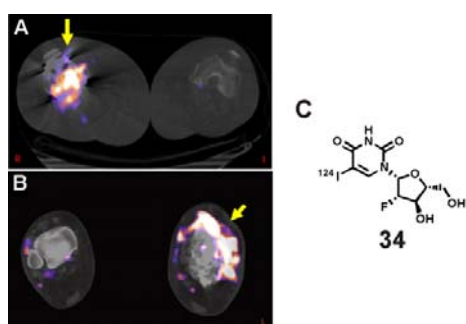
Figure 3. PET/CT scans of septic arthritis (MRSA) in the right knee (a) and cellulitis (multiple bacterial strains) in the left lower extremity (b) 2 hours after IV injection of 74 MBq of [^{124}I]FIAU. (Reprinted from Diaz. Et al. PLoS ONE 2007, 2(10), e1007)
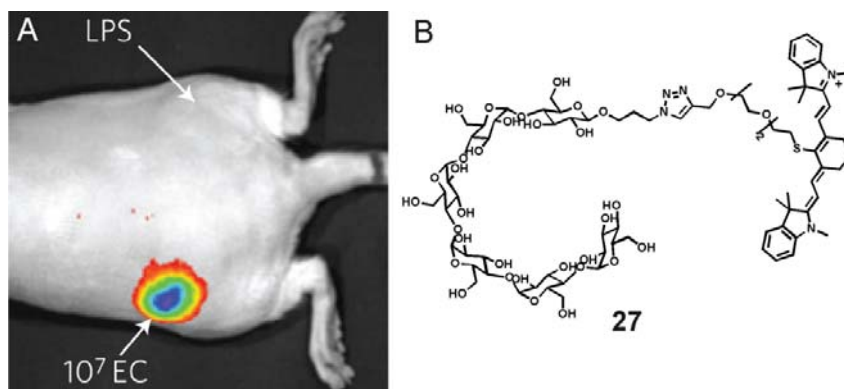
Figure 4. a) Discrimination between a an E. coli infection and an LPS induced inflammation in a rat model (a) 16 h after IV injection of 280-350 μL of a 1mM solution of IR786-labeled maltodextrin (b). - (Reprinted by permission from Macmillan Publishers Ltd: Nature Materials, 10(8), 602-607, copyright (2011))[94]
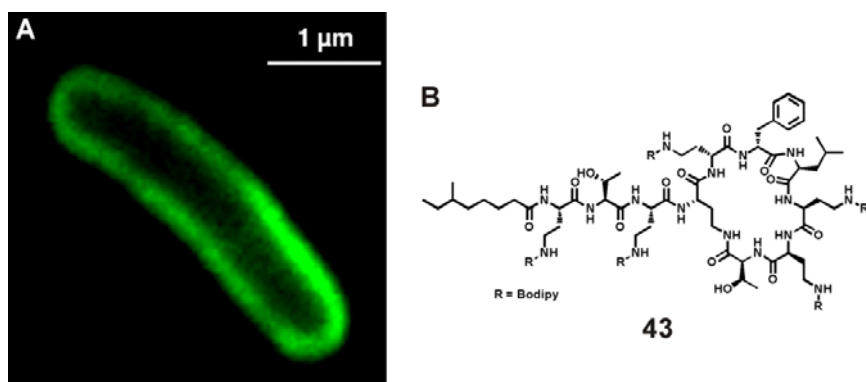
Figure 5. Confocal microscopy images of E. coli (a) incubated with 0.1 µM of bodipy-labeled polymyxin B (b). (Antimicrobial Agents and Chemotherapy, 2009, 53, 3501-3504, 10.1128/AAC.01620-08, reproduced with permission from American Society for Microbiology.
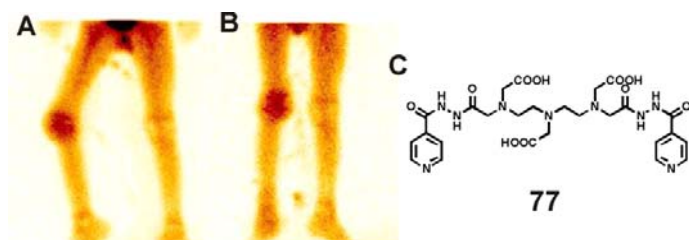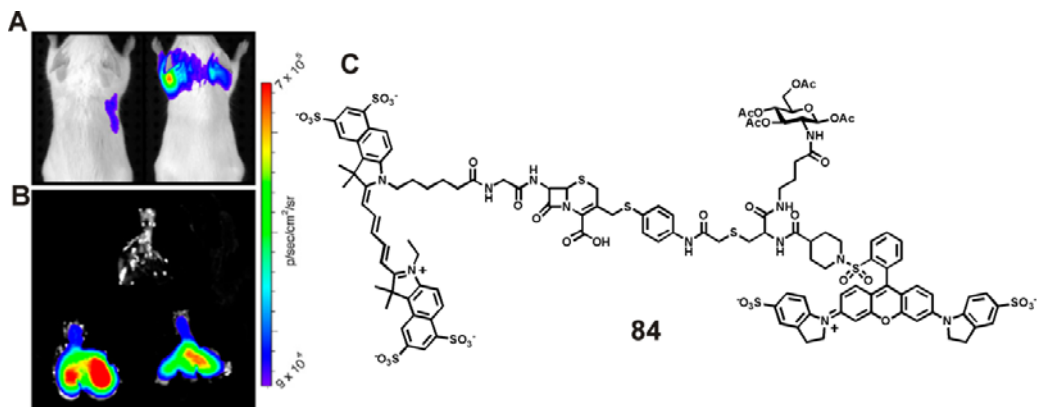

Figure 6. Whole body gamma imaging of a patient with an extrapulmonary TB infection in the right knee 1h (a) and 4h (b) after injection of 555 MBq of ^{99m}Tc-DTPA-bis(INH) (c). (Image reproduced from Hazari et al.[146])

Figure 7. A healthy and M. tuberculosis infected mouse (A) injected IV with 5 nmole of compound **84** (C) 48 post infection and injection. The lungs of the uninfected (upper) and infected (lower) mouse were scanned ex vivo for the presence of activated tracer **84** (B) (image taken from Kong et al.).[182]
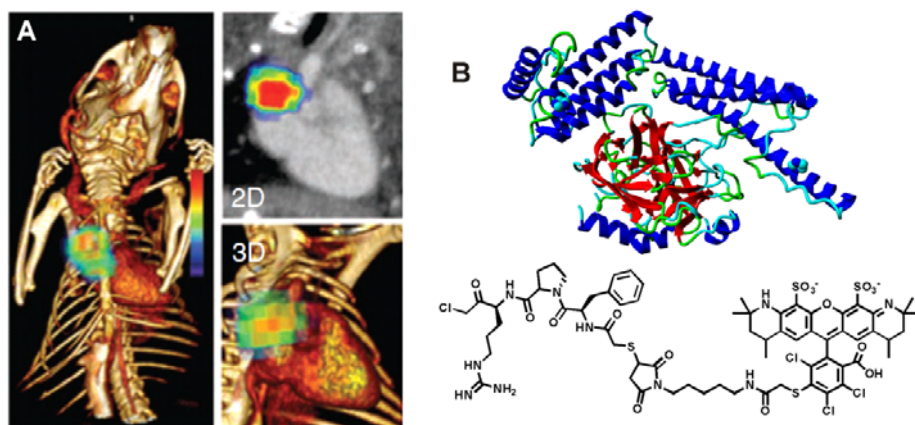
Figure 8. Optical imaging (FMT-CT) of mice with endocarditis. Coagulase-positive S. aureus are present in the ascending aorta (a). Image taken 24 h after injection of 25 μg of prothrombin labeled with AF680 via an inhibitory peptide (b). (Reprinted by permission from Macmillan Publishers Ltd: Panizzi et al., Nature Medicine, 17, 9, 1142-1146, copyright 2011)

Table 1. Prominent bacterial infections and their occurrence

Disease	Main bacterial cause	Location	Cases/year	Ref
Pulmonary Tuberculosis	M. tuberculosis (+/-)	Pulmonary	9.4 million[a]	1
Meningitis	Various	Brain and spinal cord	4.000[b]	3
Infective endocarditis	S. aureus (+)	Heart	15.000[b]	4
Fever of unknown origin	Various	Undefined		
Orthopedic infection (prosthetic)	Mainly S. aureus (+)	Prosthetic	700[c]	5
Post-interventional infection	S. aureus (+)	Surgical wound	11.7 million[a]	6

[a] Global, [b]North-America, [c]UK

Diagnostic
signal

Bacterial-specific
imaging tracer

Bacterial
infection